

**Design, Analysis and Manufacture of 2011
REV Formula SAE Vehicle Chassis**

Jacob I. Salter

20247771

School of Mechanical and Chemical Engineering
The University of Western Australia

Supervisor: Associate Professor Adam Wittek

School of Mechanical and Chemical Engineering
The University of Western Australia

**Final Year Project Thesis
School of Mechanical and Chemical Engineering
The University of Western Australia**

Submitted: October 17th, 2011

Project Summary

Torsional stiffness and weight are the two most important quantifiable aspects to the chassis of any race car. Thus, the first aim of this project is to design a chassis of which the trade-off between high torsional stiffness and low weight is balanced to achieve high vehicle performance across the various competition events. The chassis will have to comply with the specification in the Society of Automotive Engineers (SAE) 2011 Formula SAE Rules. The car, that is to be an electrically power vehicle with four hub motors has a differing set of major component than the traditional combustion engine cars in the FSAE, namely the presences of two large battery boxes and the lack of a solid engine block . The second objective is use a finite element analysis and computer aided design software, to calculate the mechanical chassis properties of weight and torsional stiffness, then comparing them against values measured from the fully fabricated chassis. To eliminate possible sources of error in the modelled values, mechanical testing of materials used in the construction will be conducted.

ACKNOWLEDGEMENTS

Swan energy is to be acknowledged for their sponsorship of the REV FSAE team by providing vital fund to purchase materials and equipment required to manufacture and construct the chassis. Acknowledgement must also go to the other members of the REV team for their hard work and commitment to the project, and to Dr Thomas Braunl for his professionalism and work ethic that has ensured the REV FSAE project got off its feet. As this thesis is being conducted in conjunctions with Brendan Waterman's thesis to produce the chassis, all of his work and contribution must be acknowledged, with citations provided in the necessary areas.

TABLE OF CONTENTS

Letter of Submission	iii
Acknowledgements	iv
Table of Contents	v
List of Figures	viii
Chapter 1. Introduction	1
1.1 Formula SAE.....	1
1.1.1 Rules.....	2
1.2 REV.....	2
1.2.1 2010 Electric FSAE Car trail	3
Chapter 2. The Chassis	4
2.1 History.....	4
2.1.1 Ladder Chassis	4
2.1.2 Twin Tube Chassis	5
2.1.3 Multi- Tubular and Spaceframe Chassis	5
2.1.1 Stressed skin and Monocoque.....	7
2.1.2 Other.....	7
2.2 The Modern Race Car Chassis	9
2.3 Deformation modes.....	10
2.3.1 Longitudinal Torsion Mode a.....	11
2.3.1 Vertical Bending Mode b	11
2.3.2 Horizontal Bending Mode c	12
2.3.3 Horizontal Lozenge Mode d	12
Chapter 3. The FSAE Chassis	13
3.1 Chassis Types Used.....	13
3.1.1 Space Frame	13
3.1.2 Monocoque.....	14
3.2 Rules.....	14
3.2.1 Standard.....	15
3.2.2 Alternative	16
3.2.3 Choice.....	17
3.3 2010 REV CAR.....	17
3.4 Suspension.....	18
Chapter 4. Vehicle Dynamics	19
4.1 FSAE race conditions.....	19
4.1.1 Acceleration	19
4.1.2 The Skid Pad	20
4.1.3 Autocross.....	20
4.1.4 Endurance.....	20
4.2 Weight transfer.....	20
4.2.1 Lateral Weight Transfer	21
4.2.2 Longitudinal Weight Transfer	21

Chapter 5. Design Methodology and Criteria	22
5.1 Design Criteria	22
5.1.1 Battery boxes	23
5.2 Torsional stiffness	23
5.3 Design Tools	24
5.3.1 Solidworks	25
5.3.2 Ansys	25
5.4 Process Flow	26
5.4.1 Improvements	26
5.4.2 Chassis design iterations	27
5.4.1 Chassis sections	28
5.4.2 Scaled Deformation Results	29
5.4.3 Battery boxes and stressed skin floor	29
Chapter 6. Material and Tubing Selection.....	30
6.1 Section Properties.....	30
6.2 Tubing Supply	31
6.2.1 Allowable vs. purchased	31
6.2.2 Cost and weight	32
6.1 Material Testing	32
6.1.1 The Test Rig	33
6.1.2 Sample preparation.....	33
6.1.3 Method	34
6.1.4 Results and discussion.....	35
6.1.5 Conclusion.....	36
Chapter 7. Chassis Evaluation	37
7.1 Finite Element Analysis	37
7.1.1 Boundary conditions and loads	37
7.1.2 ANSYS.....	38
7.1.1 Solidworks Simulation	40
7.1.2 Torque Calculations	40
7.1.3 Mesh Refinement	41
7.2 Physical Testing.....	42
7.2.1 Testing Procedure.....	42
Chapter 8. Project Safety.....	44
8.1 Construction	44
8.2 Physical testing of the chassis	44
8.3 REV Lab.....	45
8.4 Chassis of a Race Car.....	45
Chapter 9. Results and Discussion.....	46
9.1 The Design	46
9.1.1 Tubing properties	46
9.1.2 Rules.....	47
9.1.3 Weight	47

9.1.4	Torsional Stiffness.....	47
9.1.5	Comparisons.....	48
Chapter 10. Conclusion		50
Chapter 11. Future work and recommendations		51
11.1	2013 REV FSAE Chassis.....	51
11.1.1	Material	51
11.1.2	Chassis Type	51
11.1.3	Battery Box integration	52
Chapter 12. References		53
Appendix A. Tubing Type Layout		55
12.1	Tubing Type ‘A’ Diagram	55
12.2	Tubing Type ‘B’ Diagram.....	55
12.3	Tubing Type ‘C’ Diagram.....	56
Appendix B. Macro code		57
Appendix C. Performance Result of Various Racing Chassis		59
Appendix D. FEA Contour Plot of Chassis with Battery Boxes		60

LIST OF FIGURES

Figure 1: Wheel Hub Assembly (Kiszko, 2010).....	1
Figure 2: REV's Electric Lotus Elise	2
Figure 3 : 2002 UWAM Rolling Chassis (Powers, 2009).....	3
Figure 4: Ladder Chassis (Linton, 2001)	5
Figure 5: Twin Tube Lister-Jaguar Chassis (Costin and Phipps, 1971).....	5
Figure 6: Multi-Tubular Cooper Monaco Chassis (Costin and Phipps, 1971).....	6
Figure 7: Early Space Frame Chassis Lotus 19 (Costin and Phipps, 1971).....	6
Figure 8: Chassis Lotus 25/33 (Costin and Phipps, 1971)	7
Figure 9: Backbone Chassis Delorean (Wakeham, 2009).....	8
Figure 10: Tub Chassis Lotus Elise(Wakeham, 2009).....	9
Figure 11: Modern carbon fibre monocoque (Bush, 2006).....	10
Figure 12: Chassis Deformation Modes (Riley and George, 2002).....	10
Figure 13: Hybrid Chassis (Leptos, 2005)	14
Figure 14: Basic FSAE Spaceframe Chassis.....	15
Figure 15: Side Impact Structure (SAE, 2011)	16
Figure 16: 2010 REV FSAE 'Trail' Car.....	18
Figure 17: Suspension Reference geometry (Kiszko, 2010).....	18
Figure 18: Effect of Chassis Stiffness on Lateral Weight Transfer	21
Figure 19: Proposed Electrical FSAE Chassis	22
Figure 20: Simple Torsion of Shaft.....	23
Figure 21: Design Flow Chart.....	26
Figure 22: Chassis iteration A	27
Figure 23: Chassis iteration B	28
Figure 24: Chassis sections	28
Figure 25: Springs in Series	28
Figure 26: Scaled Deformation, Torsion loading.....	29
Figure 27: Schematic Instron 8501	33
Figure 28: Dog Bone Schematic	34
Figure 29: Stress Strain Graph for Test piece 2	35
Figure 30: Boundary and Loading conditions.....	38
Figure 31: Angle of twist measurement	40
Figure 32: Torque Diagram.....	41
Figure 33: FEA Mesh Refinement	41
Figure 34: Design of Physical Testing Rig	42
Figure 35: Physical Twist Angle Measurement	43

Figure 36: Final Chassis Design.....46
Figure 37: FEA Chassis' Twist under load48
Figure 38: FEA Chassis and battery boxes' under load.....48

CHAPTER 1. INTRODUCTION

This project aims to provide a Chassis for the 2011 REV electric FSAE race car vehicle, the design must comply with the rule outlined by the 2011 FSAE rulebook(SAE, 2011). The chassis will be designed using the computer aided design (CAD) program Solidworks and will be analysed using a finite element analysis (FEA) program ANSYS. By studying the design methodology used to construct previous combustion engine FSAE car chassis, it will be possible create a highly complete chassis by applying these techniques to the current design problem of an electric FASE car. The car will be run using four hub motors, with all hubs running independently thus allowing a huge potential and benefit in the area traction and cornering (Millken and Millken, 1995). Highly powerful Lithium-ion battery will be powering the hubs, and room for 60kg or 30 litres of these batteries will have to be made somewhere in the chassis.

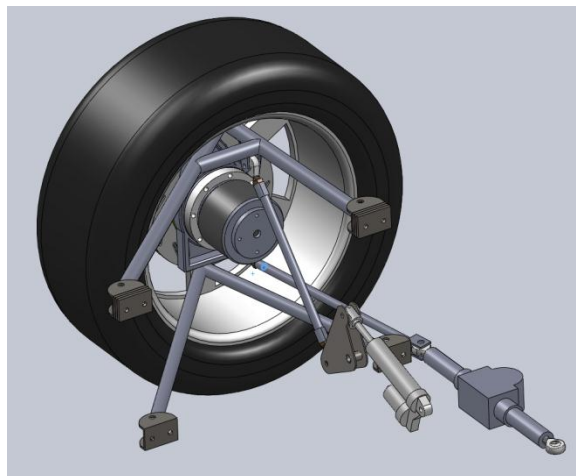


Figure 1: Wheel Hub Assembly (Kiszko, 2010)

1.1 FORMULA SAE

The Formula SAE (FSAE) competition is a worldwide platform for engineering student to practice their skill and learn new ones in a highly practical way. The competition is highly competitive with some teams acquiring large budget through sponsorship and university funding, thus most producing highly advanced cars. The UWA motorsport

Team has made their mark on the international stage by taking out the world championship in 2007.

1.1.1 Rules

The FSAE like any racing body sets out rules for the design and specifications of the cars that are allowed to compete, with all areas from seats belts standards to engines output covered in the rule books. The design and specifications for the chassis are highly regulated in order to maintain maximum safety. A number of years ago the FSAE introduced an electric division to the competition-allowing hybrid and fully electric car to enter, these car are judged using the same criteria as the traditional combustion cars and compete in the same events. The addition of the electrical cars comes with the added complexity of more rules, which are centred on maintaining safety in and round the car's electrical systems (FSG, 2010).

1.2 REV

As the push for greener and more environmentally friendly method of transportation became stronger the UWA Renewable Energy Vehicle Project (REV) was created. Over the past couple of years, the project has successfully converted a number production car to fully electric, with the latest addition being the REV's Louts Elise (Figure 2)



Figure 2: REV's Electric Lotus Elise

This sports car was chosen to break the stereotype surrounding electric cars of been small, slow and not aesthetically pleasing, a task of which the car has performed with great success. As the option to enter an electric car into the FSAE became open, it was decided that the time was right given the level of experience within the REV team

through the work completed on the Lotus and the Getz, to entering a fully electric car into the FSAE.

1.2.1 2010 Electric FSAE Car trail

In 2010 a trail FSAE electric car was constructed using the UWA Motorsport 2002 rolling chassis (frame, suspension and wheels), see figure 3. Although the chassis complied with the 2002 FSAE rules it was no longer valid as the FSAE are continuously updating their rules for safety reason, thus the car was unable to be entered into the 2010 competition. This ‘prototype’ electric FSAE car was simple rear-wheel drive car with a single battery bank, it was a good indication that the REV project was up the task of entering a car in the 2011 FASE competition.



Figure 3 : 2002 UWAM Rolling Chassis (Powers, 2009)

CHAPTER 2. THE CHASSIS

The chassis is the broad term that is used to define the frame of a car that connects all the components together. There are many different types and materials used to create a chassis, with the car's use being highly influential in selection process of these aspect. Depending on the car's weight, stiffness and cost targets, various materials and chassis types combinations will be more suitable than others, for example a carbon fibre monocoque although it may have the required weight, the cost could not be justified for a small production car using current construction methods.

2.1 HISTORY

The earliest form of a chassis dates back to the first two wheeled cart or wagon, which consisted of a simple solid axel and frame, these suspension-less vehicles are possibly even too basic to define their chassis. Once vehicles started developing suspension systems, the chassis was easier to define and was simply the frames that connected the suspension on the four corners together. The major development of the chassis was powered by the racing industry, with the teams having to be being and innovative to get the edge on their opponents. The post-World War Two Formula One competition brought the racing chassis into the twenty first century with the now highly complex composite material monocoque chassis, which was introduced in 1981 my McLaren (Bush, 2006).

2.1.1 *Ladder Chassis*

The basic ladder design was simple, easy to construct and functional, Figure 3 depicts typical a ladder chassis with its two main parallel beams and variety of cross member to complete the ladder like structure, thus its name. These chassis were used up until the mid-1930s in the racing scene (Costin and Phipps, 1971), with some industrial vehicles like trucks and utilities still using this as the basis of their chassis today. They were designed for functionality and provided little torsional stiffness.



Figure 4: Ladder Chassis (Linton, 2001)

2.1.2 *Twin Tube Chassis*

The twin-tube chassis was a developed form of the ladder chassis, with the main beams having been replaced with large tubes of which were then brace with many smaller tubes and bulkheads. Figure 4 displays the twin tube chassis of the Lister-Jaguar in 1958, with engine mounted in the front section of the car, the design was based around practicality which created a highly competitive car that set a new unlimited sports car lap record two years after its introduction (Costin and Phipps, 1971)

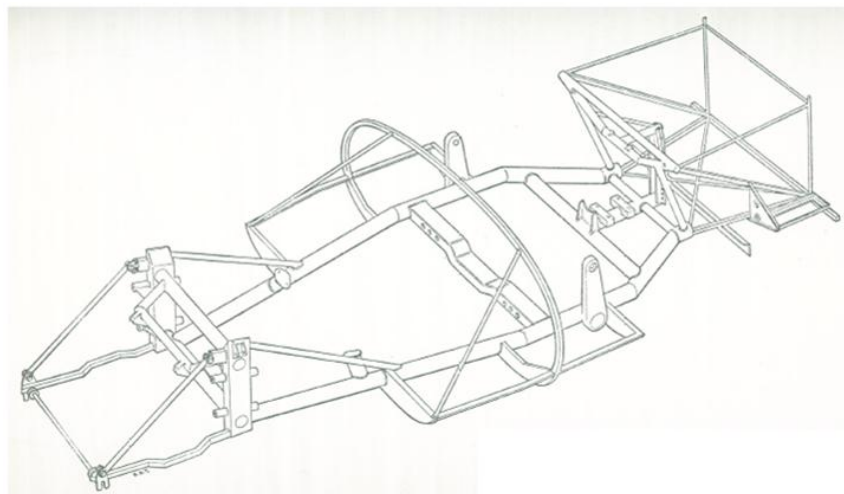


Figure 5: Twin Tube Lister-Jaguar Chassis (Costin and Phipps, 1971)

2.1.3 *Multi-Tubular and Spaceframe Chassis*

The Cooper Monaco of 1960 used a multi-tubular design, an adaption of the twin tubular design discussed above, the chassis is based around the use of four tubes running the length of the chassis. The design provided little torsional stiffness mainly

because of its lack of bracing, with the only stiffness provided primarily by the section properties of the four main tubes.

The spaceframe design was the next logical progression from the multi-tubular design with most of its members having similar section properties, thus creating a uniform framed, opposed a few main members braced by vastly smaller tubing. The main design methodology is to connect members at nodes, thus reducing the potential for bending stresses, a method utilized in the construction of truss bridges. The Lotus 19 (figure 6) was one of the most advanced sports cars of its time at its introduction, with the integration of two bulkheads into its spaceframe, a revolutionary design changing the racing game by providing vastly superior torsional stiffness. This increased stiffness proved to be the key to perfecting suspension designs and thus providing increased handling performance (Costin and Phipps, 1971).

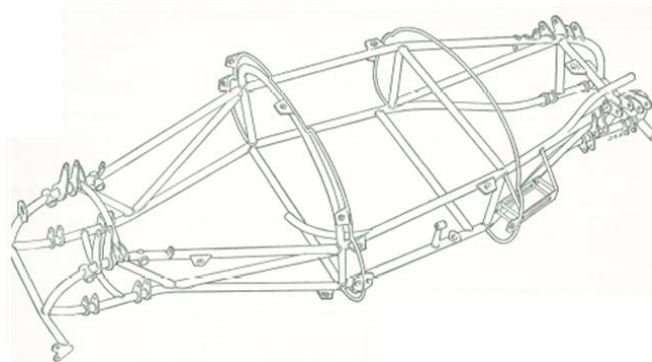


Figure 6: Multi-Tubular Cooper Monaco Chassis (Costin and Phipps, 1971)

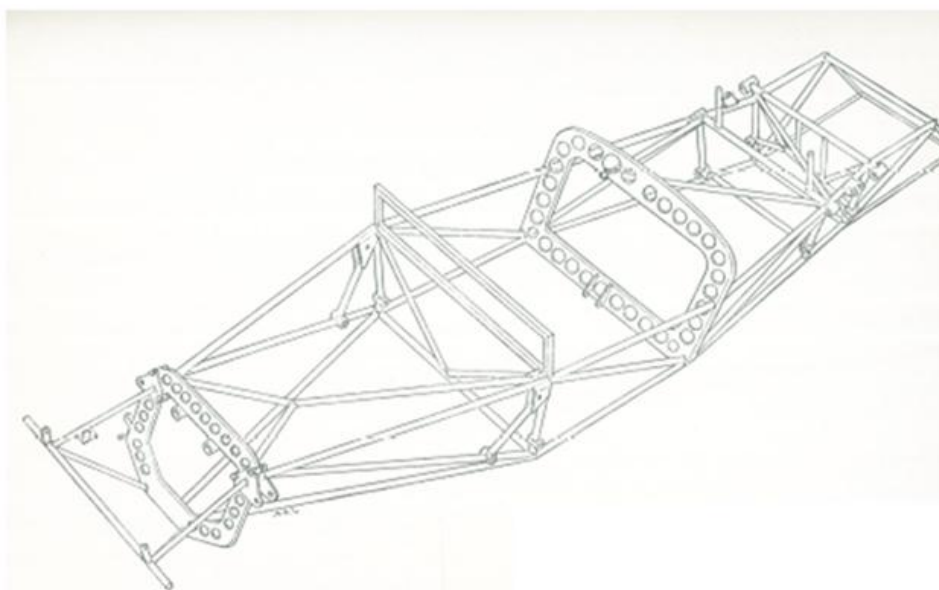


Figure 7: Early Space Frame Chassis Lotus 19 (Costin and Phipps, 1971)

2.1.1 *Stressed skin and Monocoque*

In the 1962 Formula 1 season the field of chassis design was revolutionized once again with the introduction of the Lotus 25, with its stressed skin design or as defined by (Arid, 1997) a semi-monocoque. The Lotus 25's chassis shown in figure 7 consisted of two skinned frames that extended the length of the chassis in effect making it a twin tube design although provided superior torsional stiffness than any of the twin tube design previously, (Costin and Phipps, 1971). Many teams quickly adopted this semi-monocoque design over the next few years, with the transition into a true monocoque been achieved with the introduction of the aluminium honeycomb sandwich, which combined the frame and skin of semi-monocoque into one section. The introduction of the carbon fibre composite monocoque in 1981 completed the major technological advancement in chassis design at the top level to date, with only resin and fibre changes advancing the chassis technology.

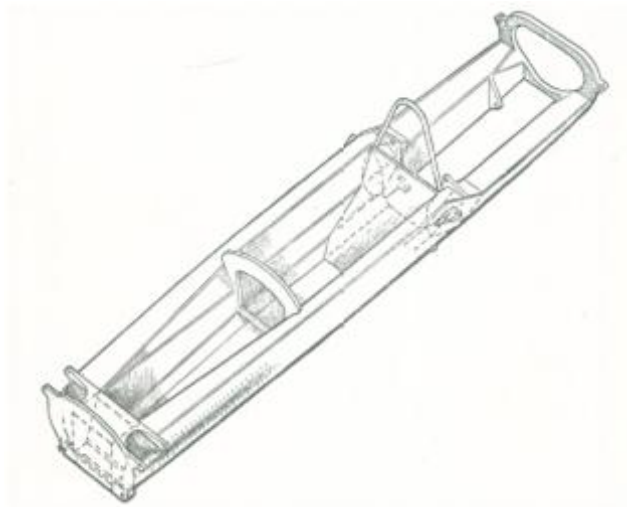


Figure 8: Chassis Lotus 25/33 (Costin and Phipps, 1971)

2.1.2 *Other*

Although they are not popular with top level racing competitions, there are some chassis type that merit a mention, for example the back bone design as present in Back to the Future's DeLorean pictured in figure 8. The design provide no inherit side impact structural for safety, but it does however meet the design criteria for the car's use. An

important fact that must be revisited when making major design choices for the 2011 REV FSAE chassis, as having any excess mechanical properties than is required is normally equates poor engineering. The back bone design did however produce respectable stiffness to weight ratio with the 1968 STP Indy turbo car and the 1962 Lotus Elan (Arid, 1997), appendix A compares this ratio of various cars of different chassis types.



Figure 9: Backbone Chassis Delorean (Wakeham, 2009)

The chassis of the REV's very own Lotus Elise is in a way similar to the stressed skin/twin tubular design of the lotus 25, although it employs multiple glued aluminium extrusions reinforced by a front and rear bulkhead (figure 9). By having the tub shallow and wide, the Elise can still be sufficiently rigidly whilst maintaining a low ride height and roof less construction (Wakeham, 2009)



Figure 10: Tub Chassis Lotus Elise(Wakeham, 2009)

2.2 THE MODERN RACE CAR CHASSIS

The type of chassis used in modern racing competitions depends highly on the rules of the competition, but as a general rule most of the top range open wheeled events like Formula 1, Champ and Indy car use a composite monocoque designs. Figure 11 display a typical Formula 1 carbon fibre composite monocoque after undergoing side impact evaluation. The heavier touring cars such as the American NASCAR employ tubular frames space frames, which suit the car's geometry and dynamics (Thompson et al., 1998).



Figure 11: Modern carbon fibre monocoque (Bush, 2006)

2.3 DEFORMATION MODES

A chassis is essentially a connection of the four suspension mounting points, with its main goal being to keep these points rigidly connected relative to one another. There are four key chassis deformation modes, these change the relative position of the four suspension mounting points and thus affecting the conditions in which the suspension system was of design around. This in turn will affect vehicle handling under the given loading conditions. These deformation modes are illustrated in figure 10.

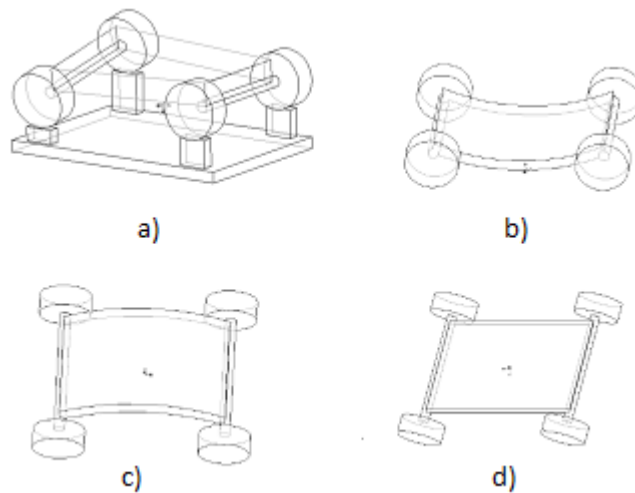


Figure 12: Chassis Deformation Modes (Riley and George, 2002)

2.3.1 Longitudinal Torsion Mode a

Longitudinal twist or torsion of the chassis is produced by diagonal loading created mainly by a cornering vehicle or bumps in the racetrack. It is the chassis' ability to resist deformation under this load that defines torsional stiffness. This property is measured in torque per unit of longitudinal rotation or twist, and it is the primary measure of a chassis' performance as it is torsional deformation that produces poor vehicle handling(Deakin et al., 2000).

2.3.1 Vertical Bending Mode b

Vertical bending is created by the weight of the drive and vehicle's components, these forces can be amplified by vertical acceleration produced from traversing a cambered track as raced in NASCAR events. As the FSAE is conducted on a flat race circuit there is no reason to design the chassis to be practically resistant to vertical bending.

2.3.2 *Horizontal Bending Mode c*

Horizontal bending will be deformation mode that the chassis in the FSAE is likely to undergo and thus should be incorporated into the design criteria of the chassis. This deformation mode is caused by the centrifugal forces created by the cornering of the vehicle, an aspect of most racing events.

2.3.3 *Horizontal Lozenge Mode d*

Horizontal lozenge occurs when the car deforms into a parallelogram like shape, this is caused by the uneven or opposing application of force on the wheels on opposite sides of the car . As the REV FSAE vehicle will be running four hub motors, it is likely that when cornering the traction control system will apply uneven power to the various wheels to maximize speed around the corner, thus creating the possibility for horizontal lozenge.

CHAPTER 3. THE FSAE CHASSIS

The FSAE competition has seen various shapes, sizes and designs of chassis roll to the starting line. A number of factors influence the decisions that the teams make when formulating their design, these include the normal performance factors of weight, stiffness and cost. Although as the FSAE encourages students to get their hands dirty and do most, if not all of the construction of the car themselves, elements such as team experience, knowledge and confidence also will influence design decisions.

Traditionally the chassis is the last piece of the design puzzle that is solved (Costin and Phipps, 1971), as it is the ‘structure’ that connects the car’s components together once they have all been designed. This unfortunately is not the case with most FSAE cars due to the period of generally a year in which the cars must be designed and built.

3.1 CHASSIS TYPES USED

There are two main types of chassis used in the FSAE, these being a space frame or a monocoque, teams make decisions based on their design criteria and restriction to what type of chassis they will use.

3.1.1 *Space Frame*

The space frame design is a very popular option for chassis type in the FSAE, as it is a low cost, simple to design and easy to construct. The design is governed by the FSAE rules, although they leaves enough freedom to see a wide verity of spaceframe shapes, sizes and design techniques. Generally there are two main options for the material used in the space frame, these are plain carbon steel and AS 4130, commonly known as chrome –moly because of its chromium and molybdenum content (Soo, 2008) . One of the main advantage of using the space frame design is its easy and logical construction process, of which can be performed by student with intermediate knowledge and experience using basic welding and metal working equipment.

Hybrid chassis have been used by a number of teams in which a simple space frame design is brace or reinforced through the uses of various panels and bulkheads (Leptos, 2005). Figure 13: **Hybrid Chassis (Leptos, 2005)** pictures the CAD designs for basic space frame chassis that is highly reinforced with carbon fibre panels.

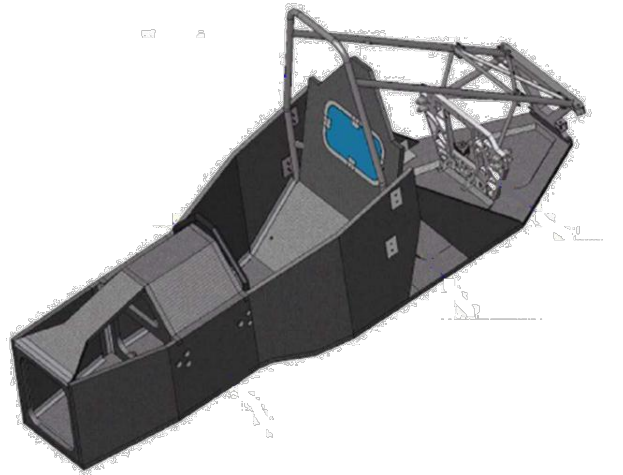


Figure 13: Hybrid Chassis (Leptos, 2005)

3.1.2 *Monocoque*

The other popular choice is a monocoque which is made usually from a composite material, with carbon fibre composite being the most popular of these choice. The construction of a monocoque is relatively simple but allows no room for error as once the ‘tub’ is set there is no going back. The rules require that the main roll hoop is to be made from steel tubing and thus a formula one style monocoque that incorporates the main intake as the roll bar is not possible under the FSAE rules (SAE, 2011). (Soo, 2008) argues that the greater cost and experience required to create a composite monocoque chassis outweighs the possible mechanical advantages, of which can be replicated by a spaceframe through smart material selection and effective triangulation.

The combination of budget requirements and team experience ruled out the use of a monocoque for the REV 2011 chassis, thus leaving a simple spaceframe as the best option for the team. By deciding to use a spaceframe, the team has the added advantage of having the trail 2010 FASE car’s chassis to study and help visualize design changes.

3.2 RULES

There are many rules that govern the design of FSAE space frame chassis, the basic structure that the rules outline is displayed in Figure 14: **Basic FSAE Spaceframe**

Chassis4. The exact dimensional layout is the job of the team's chassis designer, of which there are two 'paths' to choose from in order to produce a rule compliant chassis:

1. Using the specification for minimum tube thickness and diameter for 'controlled members'
2. The alternative rules, which use load requirements on the main structural members in that chassis.

3.2.1 *Standard*

The first option is the simpler path, figure 14 displays the 'base chassis' and figure 15 defining the side impact structure, with table 1 showing the required dimensions for the given member's cross sectional geometry. As can be seen in table 2 there are various options in each category, these slight variation in thickness and diameter allow greater possibility that teams can source the materials locally. The rest of the chassis' members that are not regulated can be as small or large as the designer desires.

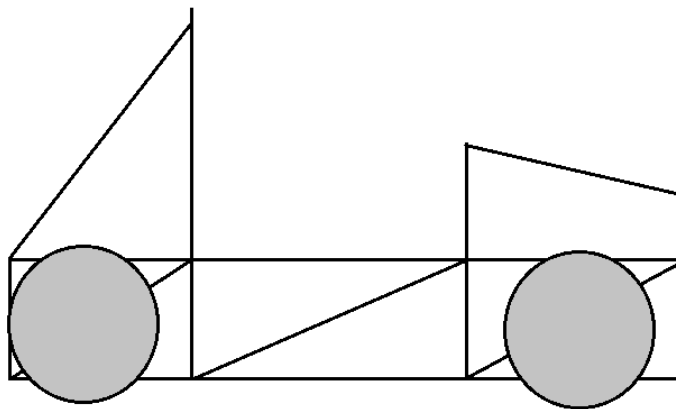


Figure 14: Basic FSAE Spaceframe Chassis

ITEM or APPLICATION	OUTSIDE DIMENSION X WALL THICKNESS
Main & Front Hoops, Shoulder Harness Mounting Bar	Round 1.0 inch (25.4 mm) x 0.095 inch (2.4 mm) or Round 25.0 mm x 2.50 mm metric
Side Impact Structure, Front Bulkhead, Roll Hoop Bracing, Driver's Restraint Harness Attachment (except as noted above)	Round 1.0 inch (25.4 mm) x 0.065 inch (1.65 mm) or Round 25.0 mm x 1.75 mm metric or Round 25.4 mm x 1.60 mm metric or Square 1.00 inch x 1.00 inch x 0.049 inch or Square 25.0 mm x 25.0 mm x 1.25 mm metric or Square 26.0 mm x 26.0 mm x 1.2 mm metric
Front Bulkhead Support, Main Hoop Bracing Supports	Round 1.0 inch (25.4 mm) x 0.049 inch (1.25 mm) or Round 25.0 mm x 1.5 mm metric or Round 26.0 mm x 1.2 mm metric

Table 1: Tubing Thickness and Size Rules (SAE, 2011)

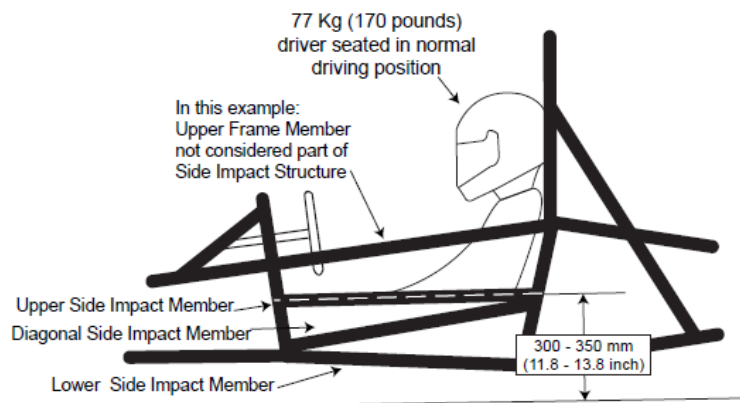


Figure 15: Side Impact Structure (SAE, 2011)

3.2.2 Alternative

The alternative rules require the use of FEA software and thus more technical work, although it allows even more freedom in the design and thus greater possibility for a better chassis that is lighter and more rigid. The cross-sectional dimensions of the space frames members can then be highly customize to optimize the chassis' design. Table 2 outlines the loading conditions a chassis is required to withstand resulting in a deflection of any point of not greater than 25mm.

Placement	Force (kN)		
	X	Y	Z
Main roll Hoop	6	5	-9
Front roll hoop	6	5	-9
Side Impact	0	7	0
Front Bulkhead	-150	0	0
Shoulder harness	0	13.2	0
Front Bulkhead off axis	-105	105	0

Table 2: Alternative rule load requirements

3.2.3 *Choice*

Given the time constraints for chassis construction the alternative rules were deemed simply too time consuming, therefore the standard rules would be used to design the chassis. This decision started the project off with a basic idea of how the finished spaceframe would look, which matched loosely then design 2010 trail electric chassis.

3.3 2010 REV CAR

As previously mention the 2010 trail REV electric FSAE car (figure16) was built using the 2002 UWA Motorsport chassis with slight modification, the idea of modifying this car to create the 2011 car by altering the chassis was proposed and investigated by (Powers, 2009). He concluded that the modifying the old chassis would not be feasible and that a completely new design would be of greater advantage as it could be purposefully built for its electrically components from the ground up. Another issue was the lack of technical information of the 2002 chassis, thus making it hard to determine if a number of the chassis' members complied with minimum wall thicknesses as outlined in table 1 above.



Figure 16: 2010 REV FSAE 'Trail' Car

3.4 SUSPENSION

The suspension of any race vehicle is a highly technical and is important to get right, the FSAE competitions has seen some very technologically advanced systems, with the 2010 UWAM team using a combination of a torsion bar and composite flexure. A design that required ten years of development to perfect. The suspension for the REV 2011 car was designed by Marcin Kiszko and presented in his thesis (Kiszko, 2010). The work was conducted from 2nd semester 2010 through to 1st semester 2011 thus suspension design was presented from very start of the chassis designing process. This provided the 20 suspension reference points as shown in figure 17, as the five internal point per corner. The chassis, as its definition outlines is then made to connect these 20 points whilst incorporating the other car components and meeting desired criteria.

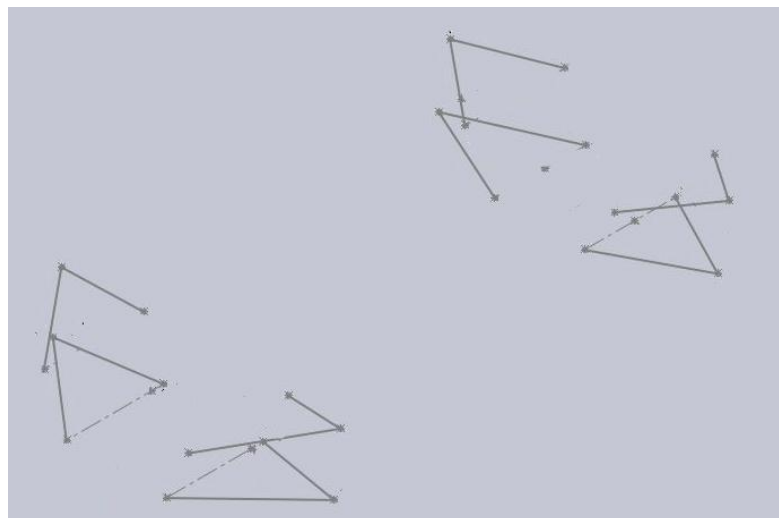


Figure 17: Suspension Reference geometry (Kiszko, 2010)

CHAPTER 4. VEHICLE DYNAMICS

The dynamics of any vehicle under the expected racing conditions dictate the loading on the vehicle and therefore the design parameters. There various factors that are important the dynamics of the car, with good handling, acceleration and breaking being the primary desirable outcome for the vehicle (Anderson and Persson, 2008).

4.1 FSAE RACE CONDITIONS

The FSAE competition is scored based on two area, static and dynamic, with both having various categories. The dynamic section consists of four events; acceleration, skid pad, autocross and endurance. The score for each of these events are outlined in table 3, with the fuel economy score being derived from the endurance event. Each of these events require something different from the chassis, it will therefore be a juggle to find the middle ground between theses varying performance criteria to achieve a maximum score.

Event	Points
Acceleration	75
Skid Pad	50
Autocross	150
Fuel Economy	100
Endurance	300

Table 3: Dynamic Event scores (SAE, 2011)

4.1.1 *Acceleration*

This event simply needs a car that can reach high speeds quickly, thus looking at Newton's second law of motion (equation 4.1), is it clear for a give force or torque provided by the motors, the car's weight is the only major factor in the equation, thus by keeping the chassis' weight to a minimum this will maximize possible acceleration. There are however number of other factors that will effect acceleration including longitudinal weight transfer which will be discussed below in sup-section 4.2.2.

$$Force = Mass \times Acceleration \quad (4.1)$$

4.1.2 *The Skid Pad*

This event is a measure of the car's cornering ability around a flat corner with a constant radius of 15.25m (SAE, 2011). The REV car is expected to perform well in this event as the combination of the traction control system with the four hub motors will produce high cornering traction and thus speed. To achieve this, the chassis is required to have a high value of torsional stiffness that is well balanced throughout the chassis, the reason for this is explained in the lateral weight transfer section below.

4.1.3 *Autocross*

The Autocross event is a standard race track sized for FSAE cars, the track comprises of a straight, constant turns, hair pin turns, slaloms, chicanes and various other turn types. Cars run on the track one at a time thus eliminating car to car interference with the average speed in the event varying between 40km/h and 48km/h. This event is designed to measure the vehicles desired performance outcomes of handling, acceleration and breaking. Scoring high will require a chassis that has a compromise between a low weight for increased acceleration and high torsional stiffness for superior cornering and handling.

4.1.4 *Endurance*

The final event is measure of the car's reliability, endurance and fuel economy, of which the first two have little to do with the chassis's performance, as they are a test of the car's drive system and fuel sources. The fuel economy however will be influenced by the car's chassis, as any superfluous weight will slow the car down thus reducing economy. With an average speed of 48-67km/h and a top speed on approximately 108km/h the desirable chassis for this event will therefore have the least possible weight.

4.2 WEIGHT TRANSFER

Weight transfer is name give the effect that lateral and longitudinal acceleration have on the load being supported by each wheel of the car, with lateral weight transfer occurring during cornering and longitudinal weight transfer present during acceleration and breaking.

4.2.1 Lateral Weight Transfer

A chassis' stiffness determines how well the vehicle deals with weight transfer around corners, this effect can be seen in figure 16 where by having a lower chassis stiffness decreases the amount of weight transfer for a give stiffness fraction. The plot also demonstrates that it is highly desire to have both front and back roll stiffness equal, this translates into a chassis that deforms at a constant rate, thus has a balanced stiffness throughout. As traction during cornering is a function of this lateral weight transfer (Thompson et al., 1998), it is desirable to design a chassis with maximum torsional rigidity. This allows the suspension to do their job correctly.

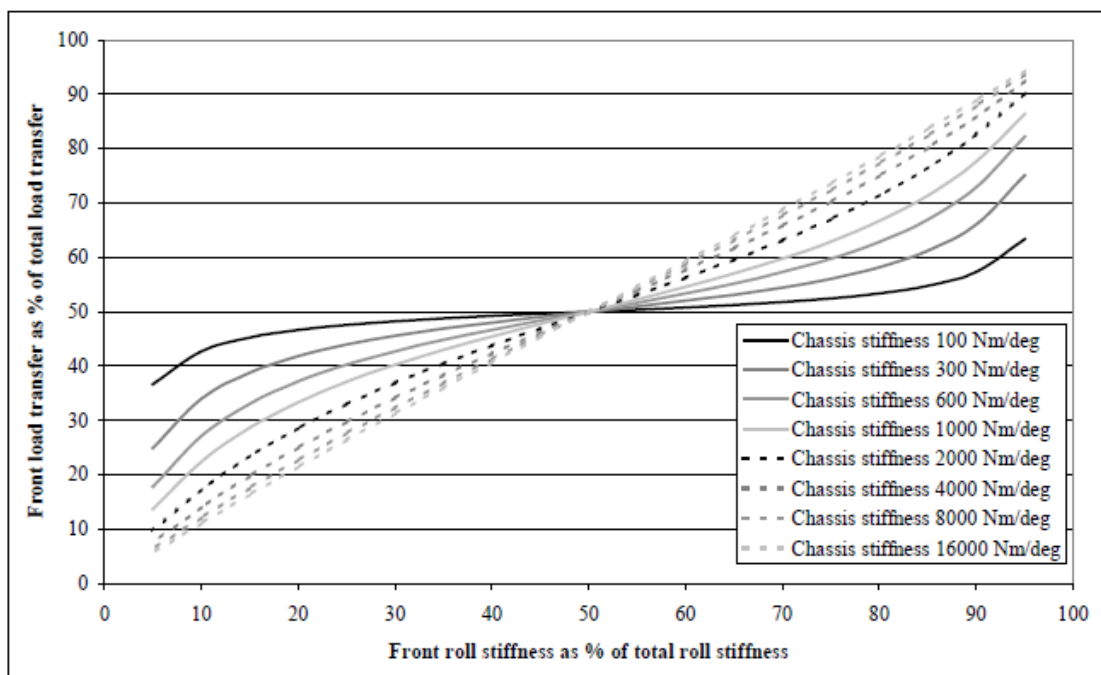


Figure 18: Effect of Chassis Stiffness on Lateral Weight Transfer

4.2.2 Longitudinal Weight Transfer

Acceleration and braking cause longitudinal weight transfer due to the longitudinal acceleration these actions induce, by having a chassis that is of sufficient stiffness the vehicle's suspension can be allowed to deal with the weight transfer correctly, which will increase the car's performance during acceleration and braking (Milliken and Miliken, 2002).

CHAPTER 5. DESIGN METHODOLOGY AND CRITERIA

The design process of the chassis consisted of many steps, from the initial assignment to the task of chassis design to the start of construction. These steps are; to identify the restriction, determine the required performance criteria, research design techniques and methodology, use CAD and modelling software to design chassis and lastly start construction. Throughout these steps, choices must be based on achieving the targets set down to meet performance requirement for condition the car will and can be reasonably expected to be subjected to under racing conditions. For example designing a rear air foil on a FSAE car that can only produce more down force than it own weight at speed greater than the car is expected to travel in competition is a futile exercise.

Figure 19 displays a proposed chassis for a purpose built electric FSAE car, the clear lack of bracing, triangulation combined with curved structural members results in a chassis with poor torsional stiffness, although producing a lighter frame. In order for this project to be deemed successful, a chassis of higher performance than the proposed will be required to be created.

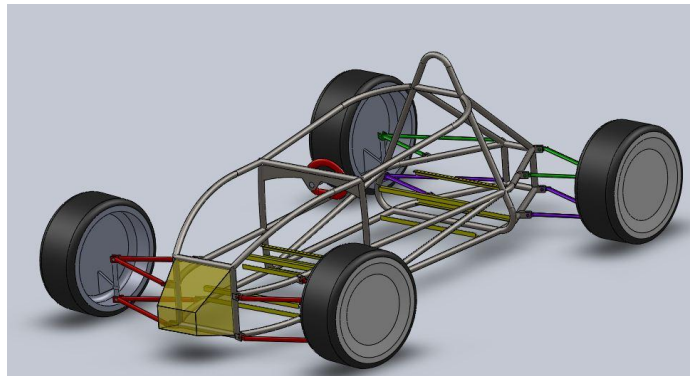


Figure 19: Proposed Electrical FSAE Chassis

5.1 DESIGN CRITERIA

The previous chapters have explained the decisions made in the various design steps so far that have shaped the design criteria. Firstly, the choice to use a space frame design that abides by the standard rules outlined in the FSAE 2011 rules book. Secondly, the required performance criteria have been identified as weight and torsional stiffness, two properties that are generally inversely proportional to one another. One downfall of the decision to use hub motors is the increased of un-sprung mass, which will increase to

forces on the chassis when the wheels are subjected to vertical acceleration (bumps) (Smith, 1984), thus the FSAE will require large torsional stiffness than normal FSAE cars.

5.1.1 Battery boxes

The position of the battery boxes was chosen as either side of the driver, they required approximately 30 litres of volume and would have to be electrically insulate from chassis. This decision was made to improve the weight distribution of the car , because the driver sit close to the back wheels ,and a four-wheel drive race car performs better with a 50:50 distribution, (Millken and Millken, 1995).

5.2 TORSIONAL STIFFNESS

In order to design a car of maximum torsional stiffness the basis or generalised equation for torsion must be examined. Figure 20 below is a basic shaft constrained at one end and an applied torque T at the other, with Φ denoting the resultant twist of the shaft.

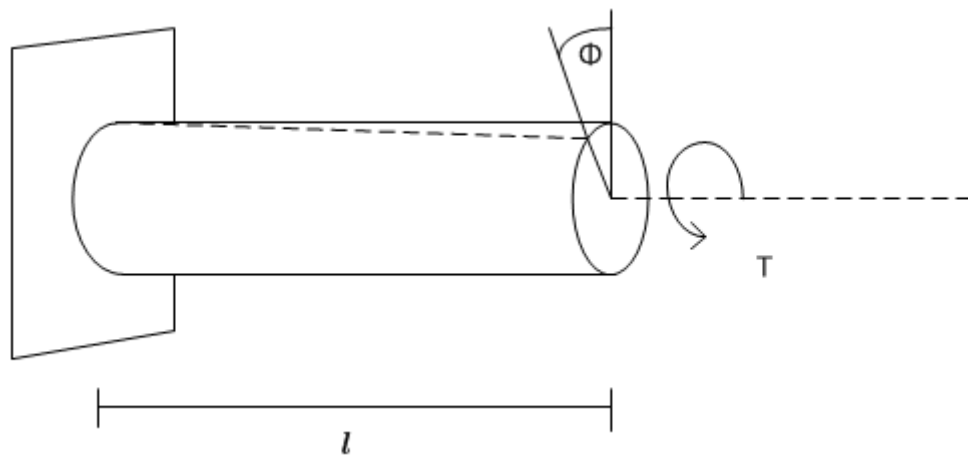


Figure 20: Simple Torsion of Shaft

Equation 5.1 is the simple formula that relates this angle of twist to the applied torque, with J representing the shafts polar moment of inertia, G representing the shear modulus of the material and l being the length of the shaft.

$$T = \frac{\Phi J G}{l} \quad (5.1)$$

This equation can then be rearranged to express torsional stiffness,

$$\frac{T}{\Phi} = \frac{JG}{l} \quad (5.2)$$

This expression displays that torsional stiffness is proportional to both the polar moment of inertia and material shear modulus, whilst being inversely proportional to the length. The stiffness of the chassis can be helped to be maximised, by using these key relationships and placing them in the context of the chassis;

1. Length – relates to the wheelbase of the car, and as it was decided to run the minimum wheelbase allowed under the rules this relationship as already been utilized.
2. Shear modulus – is related to the Young's modulus of a material and will be examined in chapter 6.
3. Polar moment of inertia – is a section property that is defined by equation 5.3 and is increased by having more cross-sectional area located further away from the neutral axis.

$$J = \int^A d^2 dA \quad (5.3)$$

The other main design approach to consider is to maintain the key basis behind a space frame design, which is to transfer all loads via nodes which ensures that load are kept axial and reducing the presents of bending in the members(Charubhun and Rodkwan). This combined with effective and efficient triangulation of the chassis can produce a space frame of similar stiffness to a composite monocoque (Soo, 2008) argues.

5.3 DESIGN TOOLS

The tools used in the design process were two engineering design software packages, which were used to firstly construct the geometry of the chassis, allowing changes to be made easily and secondly to perform FEA on the chassis to determine torsional stiffness values and to view deformation in the chassis.

5.3.1 Solidworks

The first package is Solidworks a C.A.D program with a simple user interface centred on creating various solid objects, the program has a weldmet feature which can create tubing various sized and produce complex nodal joints between the tubing by various notching options. Solidworks Simulation is an add-on for the Solidworks program that allows simple FEA of the models created in Solidworks, the transition from model to analysis is done by the simple click of a button.

5.3.2 Ansys

The second package is the FEA program Mechanical APDL (Ansys parametric design language) or commonly known as Ansys, and in comparison to Solidworks Simulation it is a highly technical and complex FEA program. The program contains options for everything from element type to mesh sizing and more.

5.4 PROCESS FLOW

The path of design work followed the flow chart in figure 21 below, as stated before the rules and performance criteria were identified, followed by Solidworks modelling and Ansys FEA. The transition of a model from Solidworks to Ansys was a complex process as there is no in-built function to input a line drawing into Ansys. The coordinates of each node had to be inputted into Ansys one at a time by hand a highly time consuming and tedious job.

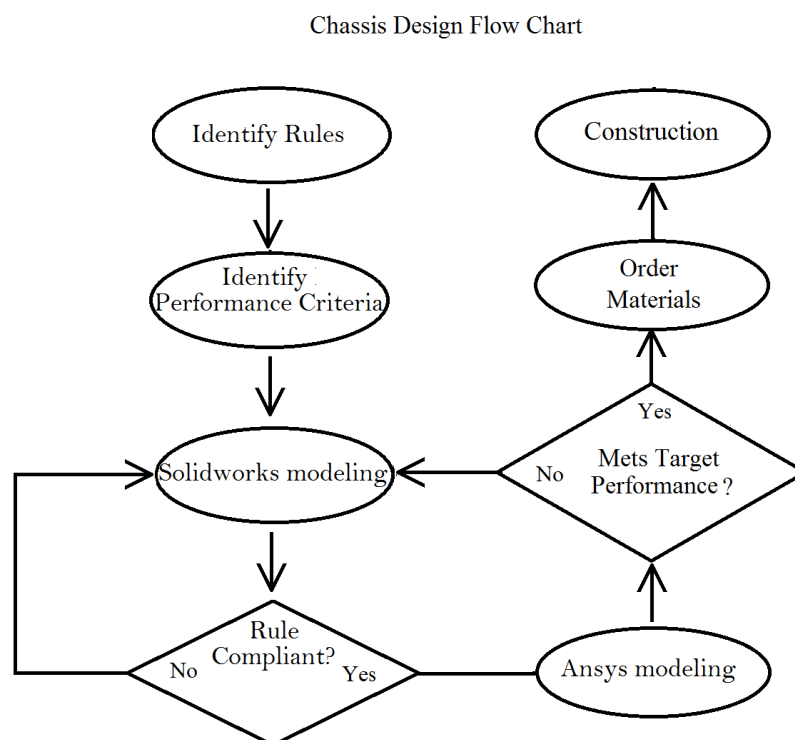


Figure 21: Design Flow Chart

5.4.1 *Improvements*

This basic flow chart was modified slightly along the way to improve speed, with the addition of Solidworks simulations FEA to replace the need for using Ansys modelling at each iteration. As to analyse a new model in Ansys would take a number of hours to input and setup, whereas Solidworks Simulation was already interfaced with Solidworks and thus took no time at all the setup and run the FEA. This did however limit the options available when performing the FEA as the program does not allow for

mesh refinement or type selection, element selection or complex loading conditions, a down side that will be discussed later.

An improvement was made to the process of transferring a model between Solidworks and Ansys. This was achieved by the creation of a Solidworks Marco (see appendix B) that exported the points in a sketch into a excel file, this data was then format into the Ansys syntax for creating a keypoint (K, key point number, X,Y,Z) and saved into a txt file. Ansys could then read from this file to quickly plot the points, which were then able to be connected up with line and produce the model, of which required only 10 minutes to perform.

5.4.2 *Chassis design iterations*

Each time a chassis would fail at one of the two junctions in the flow chart depicted in figure 21, a new iteration or chassis variation was created. Figure 22 and figure 23 display two such iterations, with each employing slightly different design techniques to achieve the performance goals. Chassis A had many square areas that required triangulation for strength, whilst chassis B attempts to incorporate the triangulation into the structure instead designing the frame and then triangulating the square sections. There were approximately twelve distinctly different iteration designs before the final design was rested upon.

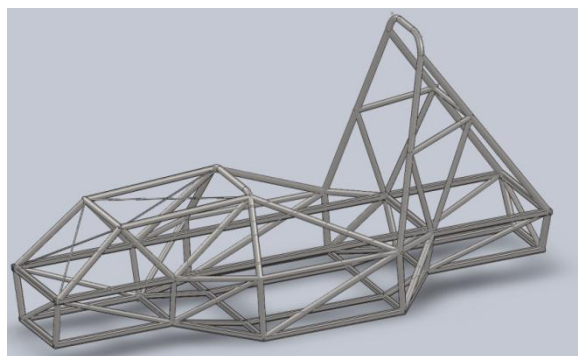


Figure 22: Chassis iteration A

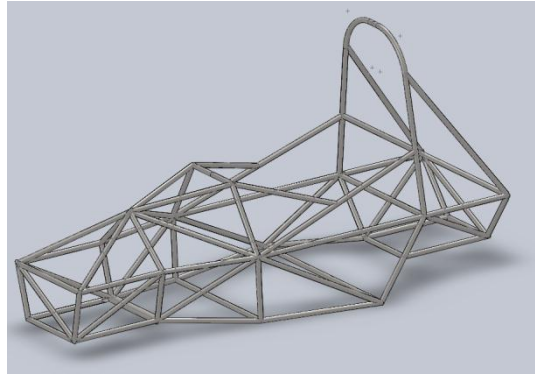


Figure 23: Chassis iteration B

5.4.1 Chassis sections

As a method for analysing and balancing the chassis, the chassis was divided into three main sections, the front bulkhead, the driver compartment and the rear section. The main and the front roll hoops were used to define the section boundaries, figure 24 shows the divisions on the base chassis.

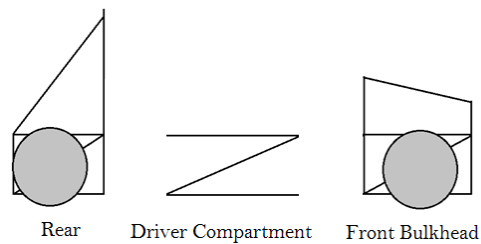


Figure 24: Chassis sections

By treating each of these sections as one of three springs in series (figure 25) and using basic spring theory equation 5.4 was derived. Upon brief examination, it can be seen that the best arrangement is to have all the springs of equal stiffness, which will maximize the efficiency.



Figure 25: Springs in Series

$$\frac{1}{k_T} = \frac{1}{k_1} + \frac{1}{k_2} + \frac{1}{k_3} \quad (5.4)$$

5.4.2 *Scaled Deformation Results*

The Solidworks Simulation software was used to create scaled deformation contour plots, which applies a scale factor to the deformation created by a load applied to the chassis. Figure 26 shows the final chassis design under load with a scale factor of 30, by examining each section as defined in figure 24, it is clear that the driver's compartment is deforming the most and is thus the least stiff, which therefore greatly reduces the total chassis torsional stiffness as calculated in equation 5.4.

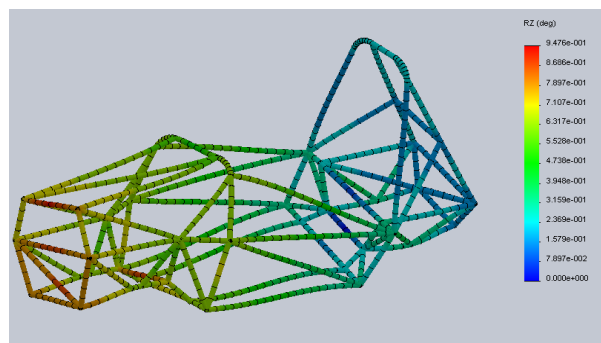


Figure 26: Scaled Deformation, Torsion loading

5.4.3 *Battery boxes and stressed skin floor*

To rectify the reduced stiffness of the driver's compartment, it was decided that the battery boxes were to be included into the modelling. They were designed to be made from 0.95mm sheet steel and would be closed in of all six faces. A stressed skin bottom was also designed into the chassis and would extend over the bottom of the drivers compartment. These added components would increase the stiffness of the central section and therefore the whole chassis. The resulting increase in torsional stiffness is discussed in chapter 9. The battery boxes, include the stressed skin floor.

CHAPTER 6. MATERIAL AND TUBING SELECTION

The decision to use a space frame design chassis that complies with the standard rules as outlined in chapter 3, makes the process of material and tubing section property selection easier. As these decisions restrict the number possible options to choose from by defining minimum sizes of the ‘controlled’ space frame members, thus only the chassis’s additional members have to have their dimensions selected by the chassis design team.

6.1 SECTION PROPERTIES

As there is both square hollow sections (SHS) and circular hollow sections (CHS) to choose from, comparing the mechanical properties of each of these sections will help with the selection of these parts. A properly triangulated space frame will ensure that the loads on the member are mainly axial thus its strength being related to the area of the section and not their geometry. However, torsional and bending moments will still be present under a chassis deforming with longitudinal torsion.

From the equation 5.2 in chapter 5 it can be seen that the polar moment of inertia (J) is the relevant section property that is proportional to torsional stiffness. When using the below two equations to calculate J for some of the difference size tubing allowable for selection, we can see the defined differences.

$$J_{SHS} = \frac{b^4 - (b-t)^4}{6} \quad (6.1)$$

$$J_{CHS} = \frac{\pi(r^4 - (r-t)^4)}{4} \quad (6.2)$$

Table 4 displays the calculated sectional properties of four of the minimum allowable members, with the last column being the ratio between the polar moment of inertia and the area of the given section, thus by the law of proportionality, the ratio between torsional stiffness and weight for a given section. It can clearly be seen that the SHS has a significantly lower ratio than the three CHS.

	Area (mm ²)	J (mm ⁴)	Ratio
26.9x2.6 CHS	93.3	105507.2	1131
25.4x1.6 CHS	61.8	74909.0	1212
25.4x25.4x1.4 SHS	60.9	12076.4	198
26.9x2.6 CHS	57.1	67265.4	1177

Table 4: Polar moment of inertia comparison

6.2 TUBING SUPPLY

An appropriate steel supplier was required to be selected base on a number of factors; firstly that they stocked the required tubing with the correct sizes, material and finish but also so that the pricing was not unreasonable.

Midalia steel was chosen for their pricing and their stock of tubing close to the right sizes that we required. All the steel tubing that was purchased complies with AS1450-Steel tubes for mechanical purposes. Plain carbon steel was selected to be the material as it is cheap and easy to working with thus allowing easier construction (Waterman, 2011).

6.2.1 *Allowable vs. purchased*

The tubing purchased from the supplier differs slightly geometrically from the minimum as required by the rules and therefore adding weight, but also increasing the section properties, table 5 outlines theses differences. Table 6 displays the polar moment of inertia of the supplied steel, the J/A ratio and its increase from the J/A of the rules defined sections. The material used is therefore not only stronger than that of the minimum but more efficient.

	Rules min		Supplied		Difference		Area increase (%)
	D (mm)	t (mm)	D (mm)	t (mm)	D (mm)	t (mm)	
A	25	2.5	26.9	2.6	1.9	0.1	12.1
B	25.4	1.6	25.4	1.6	0	0	0.0
B2	25	1.25	25.4	1.4	0.4	0.15	13.5
C	25	1.5	25.4	1.6	0.4	0.1	8.2

Table 5: Steel Tubing Supply

	Area (mm ²)	J (mm ⁴)	Ratio	Increase (%)
A	104.6	137392.1	1314.1	16.2
B	61.8	74909.0	1211.6	0.0
B2	69.2	14075.9	203.5	2.7
C	61.8	74909.0	1211.6	2.9

Table 6 : Steel tubing supply properties

6.2.2 *Cost and weight*

The cost and weight of the ordered materials are outlined in table 7 below, the data was taken from the material supplier and gives a reasonably accurate value for the chassis' final weight. The reason for the additional 20% in ordered length was to allow for mistakes and off cuts, to try and prevent the need to order a second time, this however was required due to the incorrect bending of the main roll hoop. The raw cost of the steel was well within the chassis budget of approximately \$1000, allowing more money for other uses.

Type	Required + 20% (mm)	Unit lengths (m)	Cost/Length	Weight/length (kg)	Cost	Weight Used (kg)
A	5272.8	6.5	\$19.50	10	\$19.50	6.76
B	18576	6.1	\$25.22	5.67	\$100.88	14.39
C	16104	6.1	\$30.18	6	\$90.54	13.20
Total					\$210.92	34.35kg

Table 7: Cost and Weight of Material used

6.1 MATERIAL TESTING

A comparison is to be made between the FEA modelling result and the result of the physical testing of the chassis, so it order to try and eliminate any other possible sources of error testing was completed on steel that was used during construction. The only two material input that the FEA modelling program Ansys uses are Young's Modulus and Poisson's ratio. To verify the values of theses material properties as provided by the manufactures would hopefully reduce the error between modelled and tested result for the chassis performance. These material properties are both possible to calculate, but it was decided to test only for Young's modulus and to use a standard value for Poisson's ratio.

6.1.1 *The Test Rig*

The most readily available testing instrument was a Instron machine located on campus in the mechanical engineering building. Due to load restrictions on the on the clamps that were used to hold the testing samples, the maximum load was restricted to 5kN of the possible 50kN the Instron 8501 machine is capable of. Figure 27 below is a schematic of the Instron 8501 with the various key elements.

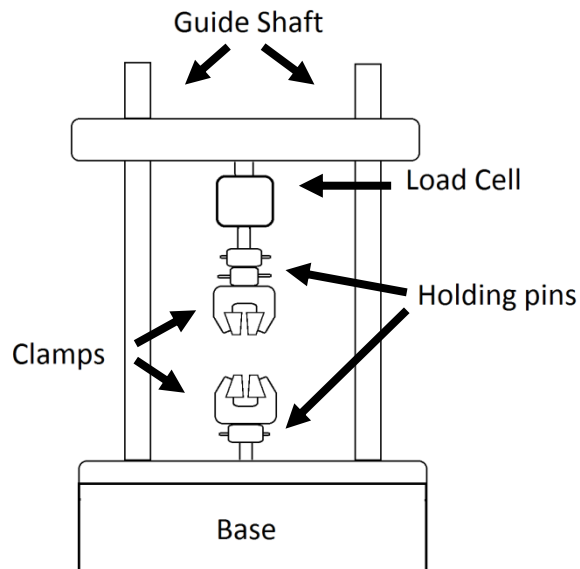


Figure 27: Schematic Instron 8501

6.1.2 *Sample preparation*

The testing three samples were made from the 25.4 x 25.4 x 1.4mm SHS used in the chassis and one from the sheet steel used to make the battery boxes. To make the test pieces a length of tubing was cut to a length of 150mm, with a bandsaw used to separate the section's faces thus creating three dog bone blanks. The desired dog bone profile was then milled from these blanks with careful attention paid to ensuring accurate dimensions. The figure 28 below displays the dimensional layout of the dog bones with table 8 quantifying these dimensions for each test piece.

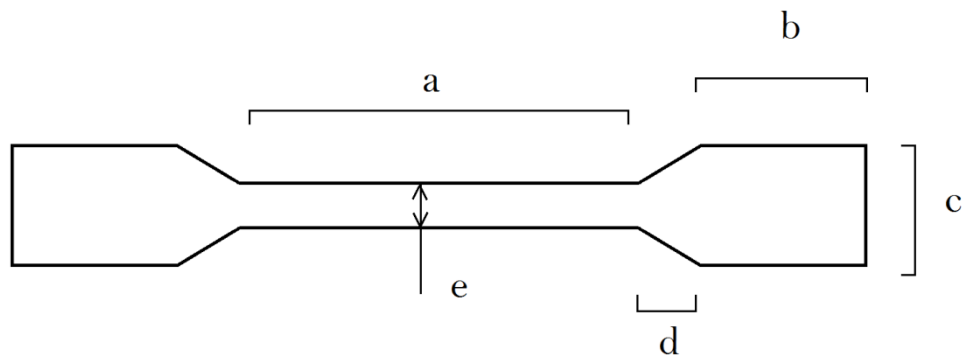


Figure 28: Dog Bone Schematic

Test Piece	a (mm)	b (mm)	c (mm)	d (mm)	e (mm)	Thickness
1	73.54	29	20	7.2	4.6	1.4mm
2	99.7	8.4	22	5.5	8.16	1.4mm
3	68.12	31.5	15.7	4	3.44	1.4mm
4	97.3	25	22	6	6.6	0.95mm

Table 8: Dog Bone dimensions

6.1.3 Method

The method used was extremely simple with the trained operator setting the various loading conditions, then securing the test pieces into the two opposing clamps and stating the operation. The computer logged the output from the Instron to a data file that consisted of force and extension values at 100millisecond intervals.

6.1.4 Results and discussion

The collected data was processed using equations 6.3 and 6.4 to derive stress and strain from the force and extension values, then using Hooke's law defined in equation 6.5 Young's Modulus could be derived from the linear-elastic section form the stress strain graph.

$$\text{Stress} = \frac{\text{Force}}{\text{Area}} \quad (6.3)$$

$$\text{Strain} = \frac{\text{Change in Length}}{\text{Length}} \quad (6.4)$$

$$\text{Young's Modulus} = \frac{\text{Stress}}{\text{Strain}} \quad (6.5)$$

The results however were difficult to interpret as the theoretical linear-elastic section of the stress strain curve for most of the test pieces were highly irregular, figure 29 displays what should be the linear-elastic region for test piece 2. It is clear that there is some source of interference, thus creating irregularities in the plot.

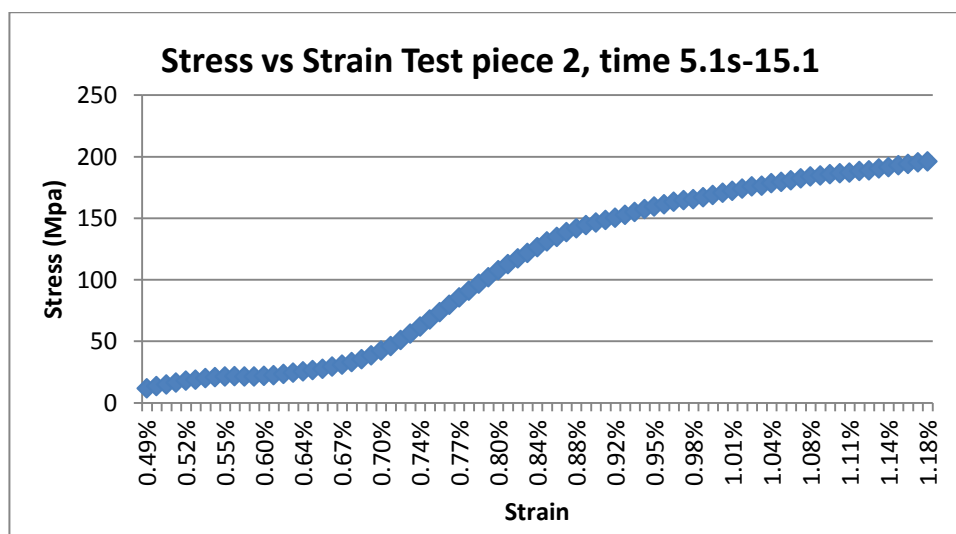


Figure 29: Stress Strain Graph for Test piece 2

Numerous sources have created this unusual plot, most of which relate to the test rig, these sources are;

- The number of components between the load cell and the stationary fixture at the base, Figure 27.

- Strain being calculated using the extension of all these ‘in-between’ components and not just the test piece.
- The angle of the clamp wedges, thus allowing the test piece to slip.
- Non-compliance to the ASTM E8 –Tension testing of metallic materials.

6.1.5 Conclusion

The material testing was unsuccessful, this is because of the various factors outlined above, by acquiring the ASTM E8 it would be possible to follow the correct procedure using approved equipment and thus derive an accurate value for the material Young’s modulus.

The value Young’s modulus as provided by the steel supplier will be used in all modelling in this thesis. This value of 210GPa is a very generic number given for most plain carbon steels. A Poisson’s ratio of 0.28 will be used.

CHAPTER 7. CHASSIS EVALUATION

The evaluation of the chassis is important as it quantifies the chassis' key performance criteria of torsional stiffness and weight, of which are then used to compare with the performance criteria of other chassis design iterations and thus rank its performance. As specified in the introduction both FEA and physical testing should be performed on the chassis to assess its performance.

7.1 FINITE ELEMENT ANALYSIS

FEA is a method used to solve a vast array of engineering problems, from heat transfer to aerodynamics and stress analysis. This is achieved by breaking up an object into a great number of basic elements, and then creating a matrix that models how these elements interact. Although it is possible to use FEA by hand for simple arrangements, the use of FEA computer software makes analysing complex structures like a space frame fast and easy.

7.1.1 *Boundary conditions and loads*

There are various different methods of modelling the torsional stiffness of a chassis, with one method type including the suspension into the analysis, whilst others do not and simply test the frame. As this thesis is centred on the topic of chassis design, the latter method type is to be used, which is a measure of the chassis frame stiffness. The technique that is to be used is a simple method that can easily be conducted in both a FEA and physical testing. For a comparison between results of the FEA modelling and that of the physical testing to be valid, all loading and boundary conditions must be the same. The red dots in Figure 30 specify the locations of the suspensions rocker mounts, it is these points that transfer the torsional loading from the wheels into the chassis. Thus they will be the location of the boundary and loading conditions for the stiffness modelling. Table 9 presents the boundary and loading conditions that will be used for all analyses both physical and virtual. UX/Y/Z denotes that the translation in the X, Y and Z direction are constrained that therefore do not move, although the three rotational degrees of freedom RX/Y/Z are not constrained and are thus allowed to change.

Position	Set value(s)
A	UX UY UZ
B	UX UY UZ
C	UX UY UZ
D	FY=Load

Table 9: Boundary and Loading Conditions

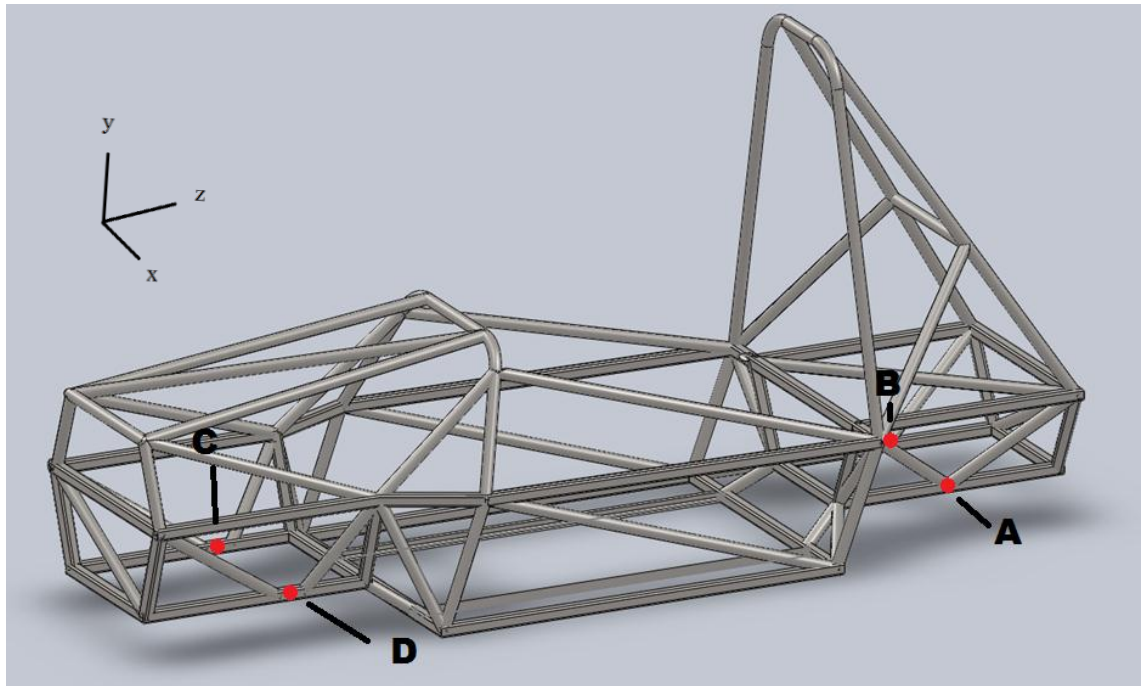


Figure 30: Boundary and Loading conditions

7.1.2 ANSYS

The reason for using a FEA software program, as mentioned in chapters five, is to compare and analyse the performance varying design iteration, with the process of transferring the model from the CAD program Solidworks to the FEA program Ansys also detailed.

The FEA of the model, once imported into Ansys is a simple process, consisting of a number of simple steps;

1. Selecting the element type(s) to use,
2. Inputting material properties,
3. Entering real constants, thickness values or section properties,
4. Meshing elements
5. Applying loads and boundary conditions,
6. Running Analysis and viewing results.

The element types selected were BEAM 181 for the tubing sections and shell element 181 being used for the battery boxes and skin floor. Ansys only required the input of Young's modulus and Poisson's ratio, with the values of 210GPa and 0.28 used respectively, these were used for both the tubing and sheet steel. The modulus value was provided by the steel manufacture and Poisson's ratio was taken from relevant literature. The beam elements need section properties, of which are derived by Ansys from the cross sectional geometry inputted by the user. These geometrical values were defined by the manufacture, of which were verified with a Vernier calliper. The shell element only required the thickness of the sheet steel, which was given as 0.95mm by the manufacture. The mesh for both the beam and shell elements is very simple, with the element length being the only option, see sub-section 7.1.3 for mesh refinement. Sub-section 7.1.1 defines the loading and boundary conditions used in the analysis.

The method for measuring the chassis twist angle due to the subjected force was done using the mid-level section of the front bulkhead. As at this point the twist angle is the very deformation that is being designed against, with the two ends being the connection points of the front suspension. The use of the simple the nodal maximum rotation data was deemed inappropriate to use as this did not represent the true angle of twist between the suspension points. Therefore the vertical displacement of the corner nodes was used to derive a suspension point relative twist angle, figure 31 illustrates how these displacements were used to calculate angle of twist Φ .

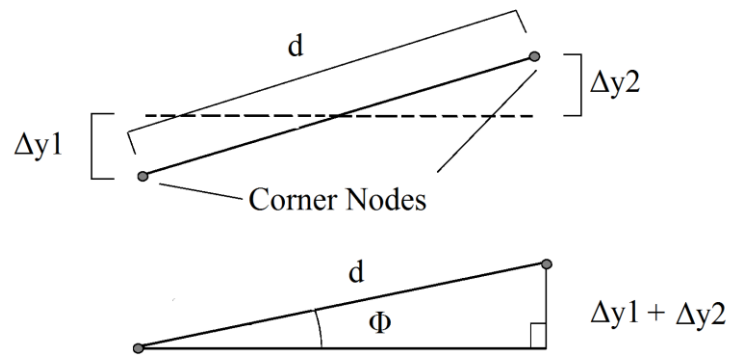


Figure 31: Angle of twist measurement

7.1.1 Solidworks Simulation

The scaled deformation contour plot used in sup-section 5.4.2 were created using the same loading and boundary conditions the Ansys analyses utilized. As Solidworks Simulation runs a highly restrictive and linear FEA, with element type and mesh being fixed by the program, the results were only used as a rough visual guide to the deformation mode of the chassis under the give loading conditions.

7.1.2 Torque Calculations

In many of the previous papers that included the chassis stiffness, the simple torque calculation were not included, which is an important as if it is incorrectly calculated the stiffness values will be wrong as well. Figure 32 below shows a simplified representation of the connection between point ‘C’ and ‘D’ as defined in figure 30. The torque on the chassis or around the axis of rotation is defined by equation 7.1 below.

$$T = Reaction \times \frac{d}{2} + Load \times \frac{d}{2} \quad (7.1)$$

By using the FEA to solve the vertical reaction force of the support, it was found that this reaction force fell between 0.2-0.8% of the applied load, thus the torque formula could be simplified to:

$$T = Load \times d$$

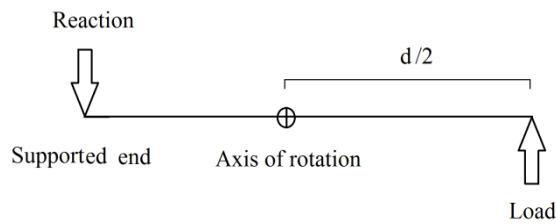


Figure 32: Torque Diagram

7.1.3 Mesh Refinement

An important process of any FEA is to refine the mesh that is used in the analysis, a process that involves reducing mesh or element size a number of times and plotting the results as to ensure the analysis is stable. Figure 33 displays the mesh refinement graph for the stiffness calculations. As can be seen the refinement percentage drops sharply to a value of 0.03%, as the stiffness value flatness off. With a mesh size of 20 mm the refinement is 0.5% which is acceptable thus this size will be used of final modelling.

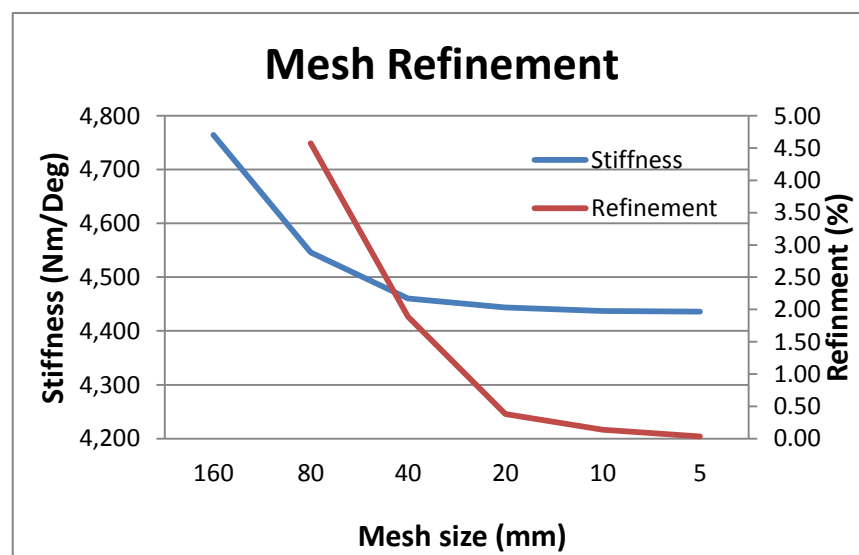


Figure 33: FEA Mesh Refinement

7.2 PHYICAL TESTING

The physical testing of the completed chassis will be highly useful as it will provide a empirical value to compare with the theoretical FEA modelling values. This will shed light on the validity of the assumption and decision that were made in order to run the FEA on the chassis design. This could also potentially highlight the slight design changes that were made during the construction of the chassis, for example inaccurate nodal joint alignment.

7.2.1 *Testing Procedure*

The setup of the physical testing will comply with the boundary and loading conditions specified in table 9, the practical application of these conditions is illustrated in figure 34. Simple chassis stands will be used to provide the fixed translation of the three support points A, B and C in figure 30. The load will be applied by attaching a steel rod through the front bulkhead of the chassis as illustrated below, with the second rear rod being used to counter acts the moments created by the first and thus stabilized the rig. The rods will rest on the bottom section of the frame between the rocker bracing members. Weights will then be added to both rods, with the resultant angle of twist and load recorded, a procedure that can be repeated to create a number of data points.

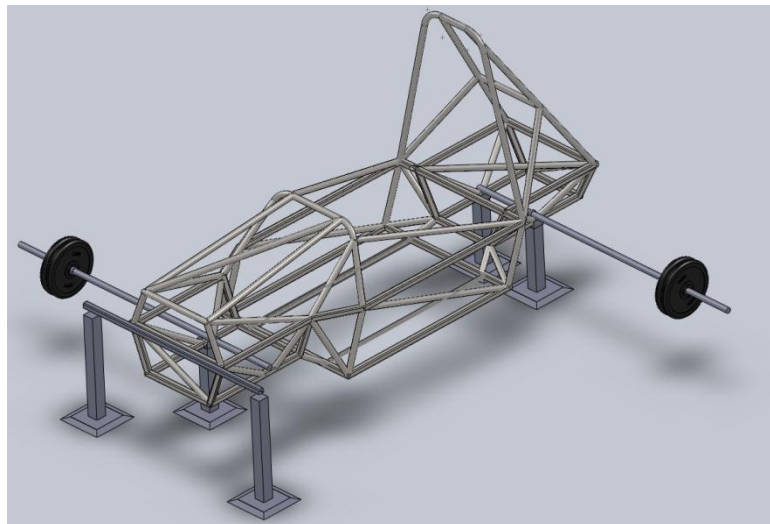


Figure 34: Design of Physical Testing Rig

The measuring of the twist angle will be made in the same fashion as that of the FEA modelling, by measuring the vertical displacement of the nodes on either side of the front bulkhead. To measure these values, a measuring rod will be attach on the front as illustrated in figure 34 and 35, with the distance between the reference stands and the ends of the measuring rod being measured with a Vernier calliper. This technique will increase accuracy of the calculated twist angle, as the longer rod will essentially magnify the displacements created thus facilitating the more accurate calculation for the angle of twist.

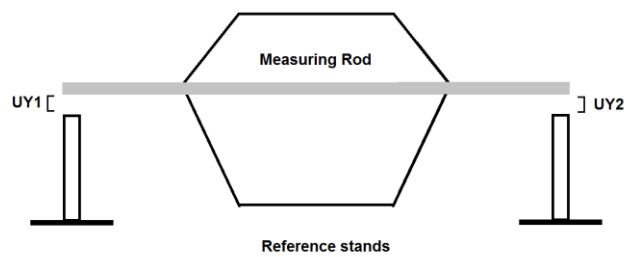


Figure 35: Physical Twist Angle Measurement

CHAPTER 8. PROJECT SAFETY

The majority of the work being done in this project is on the computer, so the only possible risks to safety in this regard will center around strains to the body and eyes due to long hours in front of a computer. There are however a number of other safety concerns that relate to various work being completed during and after the project, as well as the safety of the race car in the FSAE competition. The physical testing of the chassis will need to be completed before the chassis is used in any racing environment. This will verify that the chassis has been constructed correctly and thus safe to use by producing a stiffness values close to the FEA modeling result.

8.1 CONSTRUCTION

A potential safety risk during this project will occur through the manufacture of the chassis or scale model, which is to be conducted by REV teams members. Extensive safety check will be required to be made, including; ensure all appropriate personal protective equipment (PPE) is worn when using power tools or welder gear and with all manufacturing to be performed in a safe environment. Although there is no legal requirement for a person to have any formal welding or workshop training when utilizing such equipment off campus, only experienced and competent members will be allowed to use potentially dangerous equipment.

8.2 PHYSICAL TESTING OF THE CHASSIS

The physical testing of the chassis will be conducted after the completion of construction, and will be performed in the place of manufacture. The possible dangers and thus safety risks arise primarily round the use of heavy weights that to provide the loading on the chassis. These risks can be mitigated through the use of appropriate personal protective equipment, namely safety boot and the practice of correct lifting procedures. The potential for the chassis to fail during testing is minimal, as the loading conditions required in the test are very small and thus will produce stresses nowhere near the steel's yield stress. The only other possible factor in the testing is the failure of the welding joints, a aspect that has been addressed by the testing of weld strength and penetration of which verified sufficient strength (Waterman, 2011).

8.3 REV LAB

The FSAE team uses the REV lab for meetings and to work on our respective projects, as the lab is full of electrical equipment, a safety induction was required to be completed for lab access. As my project is working on the chassis there is no reason to be in contact with any electrical gear in the lab and therefore all the associated risks are effectively eliminated.

8.4 CHASSIS OF A RACE CAR

A designer must always help to prevent harm to the end user and any other people surrounding the designed product. This is done by ensuring that the product, in this case the chassis, will perform safely in any reasonable expectable conditions. The chassis is intended for the FSAE competition of which speeds of up to 110-120km/h can be achieved, thus a rollover or flip at these speeds although highly unlikely, must be a designed consideration. The FASE standard chassis rules can be considered as providing sufficient protection from such a roll over, as well as front ,side and rear impacts (SAE, 2011). As the final chassis design is highly braced and more robust with large tubing section properties than the base chassis as defined in the rules, it is expected that the chassis will safely protects a driver during a crash. Although, regardless of the amount of safety requirements and equipment there is always an inherit risk with participating in any high speed racing event.

CHAPTER 9. RESULTS AND DISSCUSION

9.1 THE DESIGN

A Solidworks CAD image of the final chassis design is displayed in figure 36 below, the design utilized three main type of steel, totalling approximately 32m in length. The design incorporates the battery boxes on either side of the driver's compartment, provided sufficient room for all other onboard electronics, ample room for all sizes of drivers and complies with the FSAE rules whilst attempting to posses high stiffness and low weight.

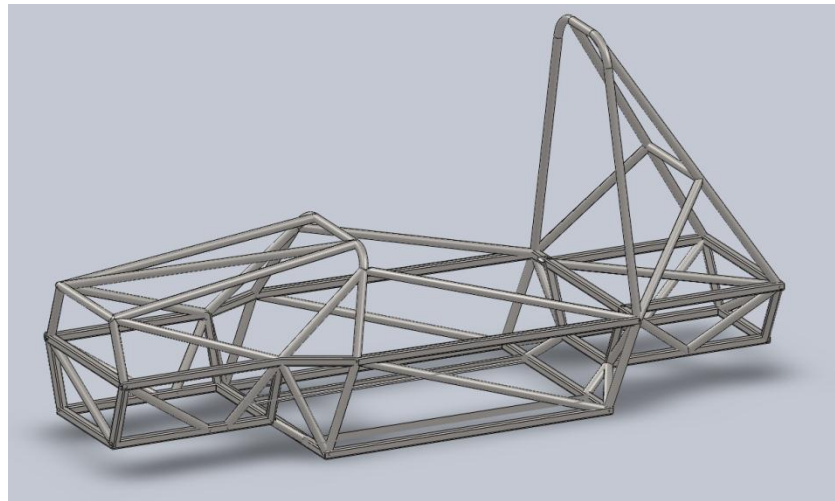


Figure 36: Final Chassis Design

9.1.1 *Tubing properties*

The final design only contained three different sizes of tubing, with table 10 below listing their cross sectional geometry. Type 'A' was used for the front and back roll hoops, with the type 'C' being used for the bottom lever perimeter, mid lever perimeter, forward most face and various connection members . Type 'B' was used for all the remaining members, refer to appendix C for tubing type diagrams.

Type	Supplied	
	D (mm)	t (mm)
A (CHC)	26.9	2.6
B (CHS)	25.4	1.6
C (SHS)	25.4	1.4

Table 10: Chassis Tubing

Although the sectional properties of type ‘C’ are far less than that of type ‘B’ (see table 6), the square cross section was beneficial for a number of reason. (Waterman, 2011) outlines these as; simple and effective suspension bracket mounts, easier construction due to self jiggling and no notching required thus saving time.

9.1.2 Rules

One of the aims of this thesis was to produce a rules compliant chassis, otherwise the car would not be allowed to compete in the competition, thus defeating the purpose of the project. Through a number of final rule checks before the construction of the chassis was started, the design was thoroughly inspected for any non-compliant aspects or components and was deemed rule complaint.

9.1.3 Weight

The weight of the chassis was calculated using Solidworks of which has a mass sensor function, by simply selecting the material type thus density the program will calculate the mass of the chassis. The weighs of the chassis with and without the battery boxes were 51kg and 37kg respectively, once again physical verification of these values will be required.

9.1.4 Torsional Stiffness

The torsional stiffness of the chassis was calculated using FEA, of which the process was detailed in chapter 7. Figures 37 and 38 plot the angular twist for varying applied torques to the chassis. The torsional stiffness can then be calculated, by simple dividing the applied torque at any point by the corresponding angle of twist. The chassis frame was calculated as 4480 Nm/Deg and 5728 Nm/Deg for the frame and battery boxes. See appendix C for Ansys FEA contour plot.

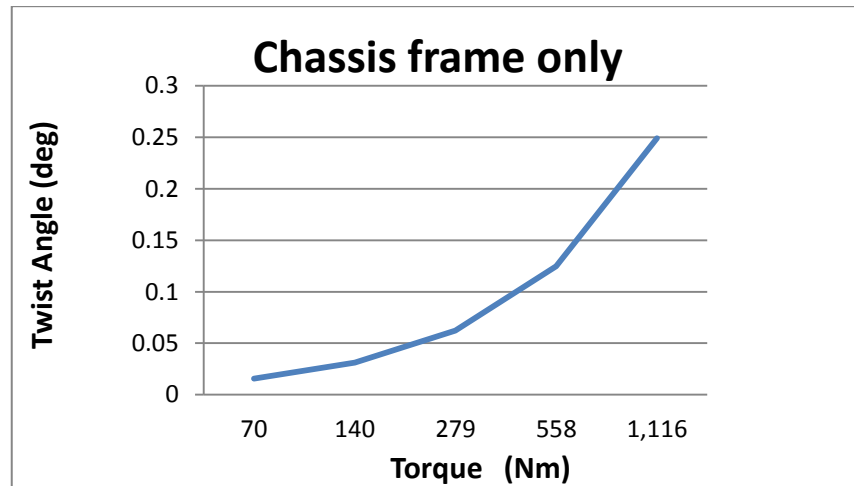


Figure 37: FEA Chassis' Twist under load

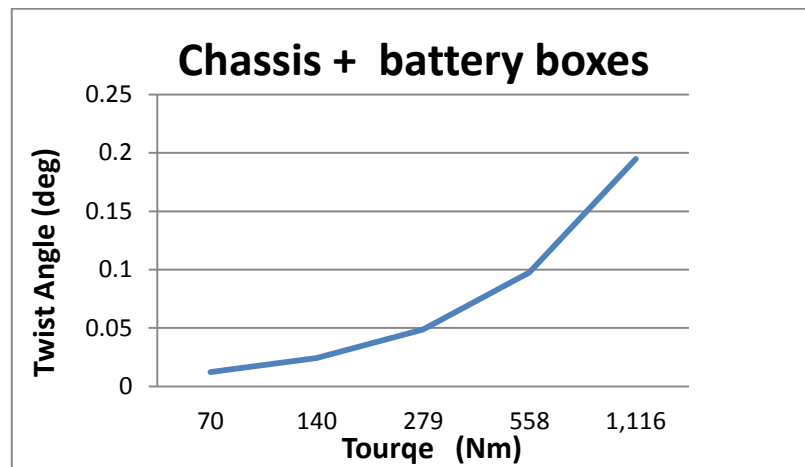


Figure 38: FEA Chassis and battery boxes' under load

9.1.5 Comparisons

Comparing these calculated values to that of previous FSAE car, would only provide basic perspective on the chassis' mechanical values of stiffness and weight, as the requirements of the electric REV FSAE chassis are different to that of combustion engine car. The setup conditions and derivations of stiffness are not the same, as some of the previous results include the suspension whilst others do not. The engine block was also included in some analyses as well, thus as the rev chassis has battery boxes instead of an engine block it is essentially useless to make a comparison. Regardless of these setup variations, out of the values presented in table 11, the REV chassis is still the stiffest, a possible necessary requirement as the unsprung weight in the REV car

will be higher than most cars due to the wheel hub assembly and thus producing a large torque during bumps.

Team	Weight (kg)	Stiffness (Nm)	Stiffness/Weight ratio
USQ '05	38	485	13.7
USQ '04	43 kg	233	5.4
Cornell '95	26	2160	83.07
REV '11	51	5728	112.3

Table 11: Stiffness and weight of previous spaceframe chassis

CHAPTER 10. CONCLUSION

The essential aim of this project was to design a chassis for the REV 2011 FSAE team, a goal that has been accomplished. Alas the construction of the chassis was not completed in time, as the chassis was only 75 % built at time of writing, and thus the car will not be competing this year's competition. The chassis' design was formulated based on techniques used previously in the FSAE and the wider racing community, the final chassis design including the battery boxes produce high torsional stiffness, valued at 5728 Nm/Deg by the FEA modelling and had a weight of 51kg. This results in a chassis torsional effectiveness of 112.3Nm/Deg/kg, of which is highly respectable when placed against that of many previous Formula 1 cars in appendix C.

As the REV car has a very different set of components, mainly two large battery boxes and hub motors than previous FSAE cars, comparison with performance data is not indicative of design quality. The lack of a standardized chassis torsional stiffness testing method, created a jumble of different values that further made comparison of chassis performance difficult. The chassis has although created a benchmark or starting point for future electric FSAE car's, as by repeating procedures in this thesis valid comparisons will be able to be made with this year's chassis and thus improvements in design will be clear. Although physical testing will need to be completed to verify the modelled values for torsional stiffness, a task also required before the chassis can be used in a car on the track.

CHAPTER 11. FUTURE WORK AND RECONNMENDATIONS

The future work that is to be done on this project would involve finishing the current chassis as to allow the team to compete in next year's competition. The physical testing should be performed on the completed chassis thus shedding light of the validity of the testing method and modelling methods in the FEA programs.

11.1 2013 REV FSAE CHASSIS

The next REV FSAE chassis will be a part of the car entering the 2013, this chassis has plenty of time to be designed and thus there are a number of area in which its design can better this year's. The design progression would follow the same path as the combustion engine vehicles, by exploring the use of different materials and chassis types. Unlike this year's design process, there will be a functional rule compliant car to base the design from, which should allow for a better performing chassis as it will be building upon the work completed this year,.

11.1.1 Material

The materials available for use in a chassis design are limited by the FSAE rules, but by exploring the use of very different material such as aluminium and composites like carbon fibre vast improvements can be made is the overall chassis performance. As one of the major design limiting factors in this year's car was cost, funding and sponsorship will need to be addressed in order to make the use of these more exotic materials feasible.

11.1.2 Chassis Type

The spaceframe is an old technology and as racing bodies like the FSAE promote the development of new and innovative designs, the exploration into a hybrid or monocoque chassis would be a good development for competition. One of the reasons why the monocoque was avoided was the lack of experience in the use of composite technology and processes amongst the team. As the REV and UWA Motorsport team are likely to merge in the coming year, the supply of knowledgeable team members in this field will be sufficient to produce a highly competitive monocoque chassis.

11.1.3 Battery Box integration

The battery boxes this year were integrated into the chassis on either side of the driver's compartment, adding to the overall stiffness of the chassis, but they have larger potential to add further stiffness to the structure. The shape of these boxes can be altered in many ways as the cells are very small, about the size of a domestic C sized battery, if designed efficiently the integrating of the battery boxes into a carbon fibre monocoque would have huge potential. (Logan, 2011)

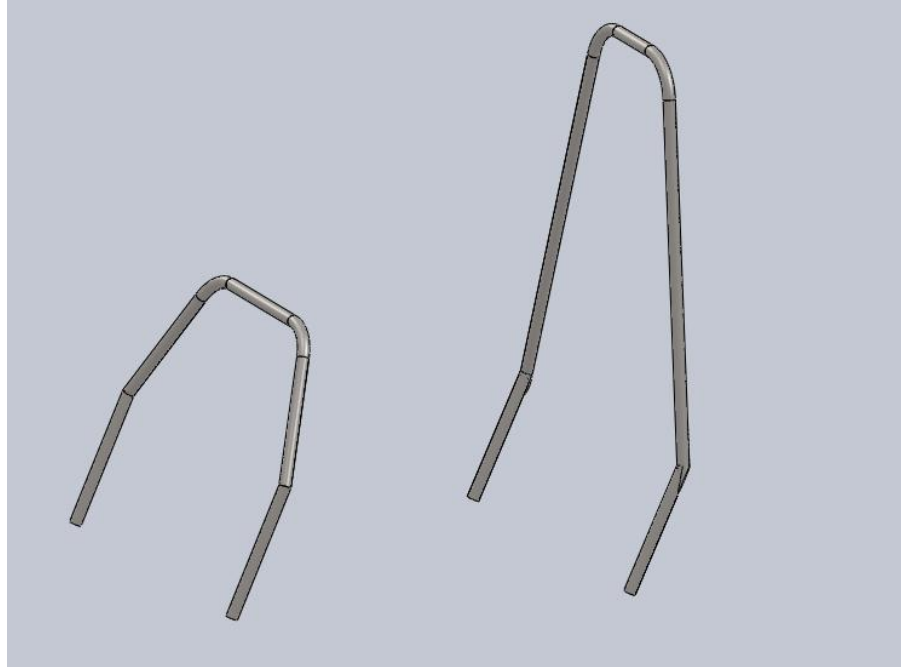
CHAPTER 12. REFERENCES

- ANDERSON, E. H. & PERSSON, J. 2008. *Analysis and Optimization of a Racecar Chassis*. Lulea university of Technology.
- ARID, F. 1997. *Race Car Chassis Design and Construction*, Osceola, Wisconsin, MBI.
- BUSH, J. 2006. Chassis type and material.
- CHARUBHUN, W. & RODKWAN, S. Design of the Space Frame Racing Car Front Clip and Rear Clip for Torsional Rigidity. Kasetsart University.
- COSTIN, M. & PHIPPS, D. 1971. *Racing and Sports Car Chassis Design*. Cambridge, Massachusetts: Robrty Bentley, inc.
- DEAKIN, A., CROLLA, D., RAMIREZ, J. P. & HANLEY, R. The Effects of Chassis Stiffness on Race Car Handling and Balance. Motorsports Engineering Conference, 2000 Dearborn, Michigan. Society of Automotive Engineers.
- ETS. 2004. Macro to read 3d Sketch points and export to Excel. *Eng-Tips Forums* [Online].
- FSG 2010. Formula student Electric Rules 2011.
- KISZKO, M. 2010. *REV 2011 Formula SAE Electric – Suspension Design*. University of Western Australia.
- LEPTOS, M. 2005. *Desgin and manufacture of Formula SAE chassis and body*.
- LINTON, W. 2001. *Analysis of Torsional Stiffness and Design Improvement Study of a Kit Car Chassis Prototype*. Master's, Cranfeild University.
- LOGAN, D. L. 2011. *A First Course In The Finite Element Method*, Stamford, CT, Cengage learning.
- MILLIKEN, W. F. & MILIKEN, D. L. 2002. *Chassis Design: Principles and Analysis*, Warrendale, Pennsylvania, Society of Automotive Egeiners, Inc.
- MILLKEN, W. F. & MILLKEN, D. L. 1995. *Race Car Vehicle Dynamics*, Warrendale Pennsylvania, Society of Automotive Engineers.
- POWERS, R. 2009. Analysis and Evaluation of the SAE Space Frame Chassis for Modification. University of Western Australia.
- RILEY, W. B. & GEORGE, A. R. 2002. Desgin, analysis and Testing of a Formula SAE Car Chassis. *SAE Motorsports Engineering Conference and Exhibition*. Indianapolis, Indiana: Society of Automotive Engineers inc.
- SAE 2011. Formula SAE rules 2011.
- SMITH, C. 1984. *Engineer To Win*, Osceola, Wisconsin, MBI.

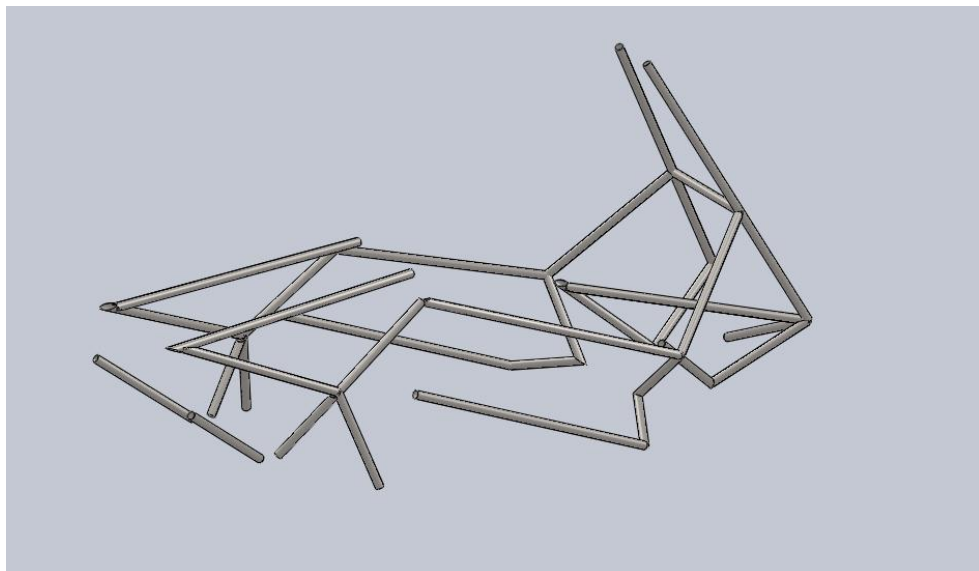
- SOO, A. M. 2008. *Manufacturing, and Verification of a Steel Tube Spaceframe Chassis for Formula SAE*. Bachelor of Science In Mechanical Engineering, Massachusetts Institute of Technology.
- THOMPSON, L. L., RAJU, S. & LAW, E. H. Design of a Winston Cup Chassis for Torsional Stiffness. Motorsports Engineering Conference, 1998 Dearborn, Michigan. Society of Automotive Engineers.
- WAKEHAM, K. J. 2009. *Introduction To Chassis Design*. Mechanical Engineering, Memorial University of Newfoundland And Labrador.
- WATERMAN, B. 2011. *Chassis Design and Manufacture*. University of Western Australia.

Appendix A. TUBING TYPE LAYOUT

12.1 TUBING TYPE 'A' DIAGRAM

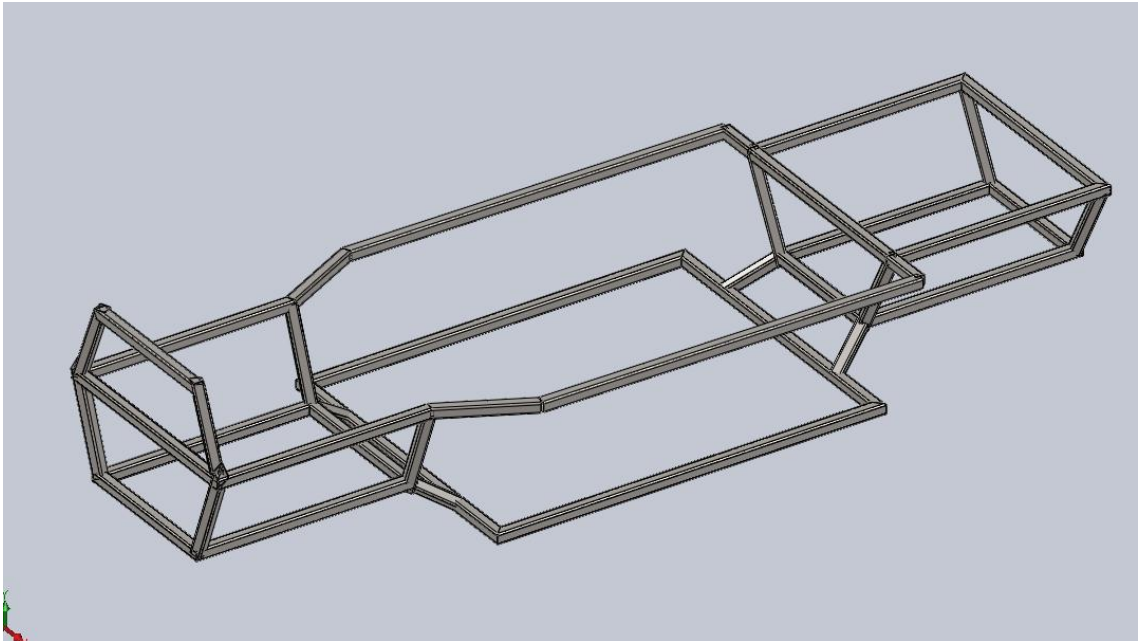


12.2 TUBING TYPE 'B' DIAGRAM



12.3

TUBING TYPE 'C' DIAGRAM



Appendix B. MACRO CODE

The code below was an adaption of code sourced from (ETS, 2004)

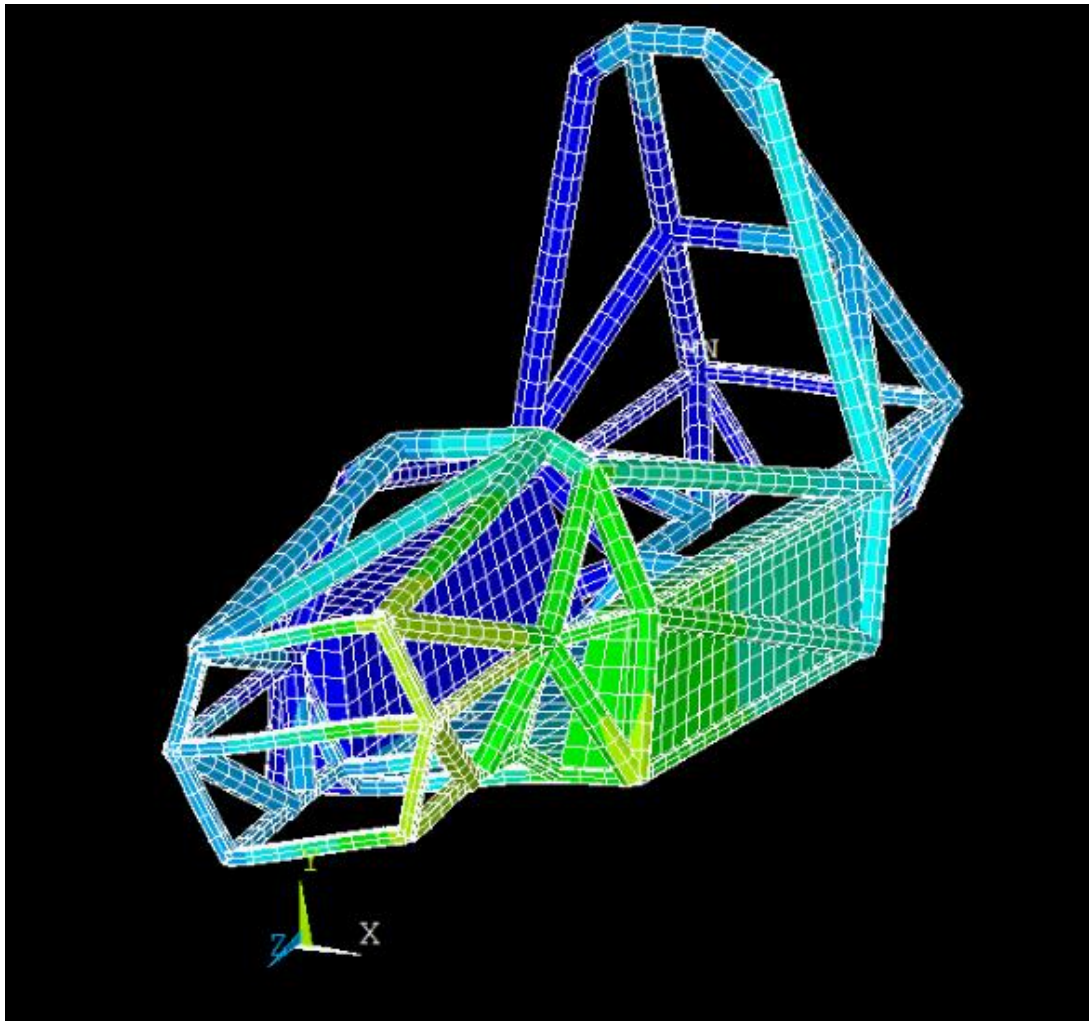
```
Sub main()  
Dim swApp As SldWorks.SldWorks  
Dim doc As SldWorks.ModelDoc2  
Dim part As SldWorks.PartDoc  
Dim sm As SldWorks.SelectionMgr  
Dim feat As SldWorks.Feature  
Dim sketch As SldWorks.sketch  
Dim v As Variant  
Dim i As Long  
Dim sseg As SldWorks.SketchSegment  
Dim sline As SldWorks.SketchLine  
Dim sp As SldWorks.SketchPoint  
Dim ep As SldWorks.SketchPoint  
Dim s As String  
Dim exApp As Excel.Application  
Dim sheet As Excel.Worksheet  
Set exApp = New Excel.Application  
If Not exApp Is Nothing Then  
    exApp.Visible = True  
    If Not exApp Is Nothing Then  
        exApp.Workbooks.Add  
        Set sheet = exApp.ActiveSheet  
        If Not sheet Is Nothing Then  
            sheet.Cells(1, 2).Value = "X"  
            sheet.Cells(1, 3).Value = "Y"  
            sheet.Cells(1, 4).Value = "Z"  
        End If  
    End If  
End If  
Set swApp = GetObject(, "sldworks.application")
```

```
If Not swApp Is Nothing Then
  Set doc = swApp.ActiveDoc
  If Not doc Is Nothing Then
    If doc.GetType = swDocPART Then
      Set part = doc
      Set sm = doc.SelectionManager
      If Not part Is Nothing And Not sm Is Nothing Then
        If sm.GetSelectedObjectType2(1) = swSelSKETCHES Then
          Set feat = sm.GetSelectedObject4(1)
          Set sketch = feat.GetSpecificFeature
          If Not sketch Is Nothing Then
            v = sketch.GetSketchPoints
            For i = LBound(v) To UBound(v)
              Set sp = v(i)
              If Not sp Is Nothing And Not sheet Is Nothing And Not exApp Is Nothing Then
                'sheet.Cells(2 + i, 1).Value = "Normal Vector " & i + 1
                sheet.Cells(2 + i, 3).Value = Round(sp.X * 1000, DEC)
                sheet.Cells(2 + i, 5).Value = Round(sp.Y * 1000, DEC)
                sheet.Cells(2 + i, 7).Value = Round(sp.Z * 1000, DEC)
                exApp.Columns.AutoFit
              End If
            Next i
          End If
        End If
      End If
    End If
  End If
End Sub
```

**Appendix C. PERFORMANCE RESULT OF VARIOUS RACING
CHASSIS**

Twin Tube	Year	Stiffness (Nm/Deg)	Weight (Kg)	Torsional effectiveness
MB W25 F1	1935	664	n/a	n/a
MB W25 F1	1937	1993	52	38
MB W25 F1	1938	2712	n/a	n/a
ERA G-type	1950	4067	n/a	n/a
Multi- tube				
Masserati F1	1957	339	n/a	n/a
Indy roadster	1955	678	68	10
Sprint Car	1995	746	75	10
Space frame				
MB W196	1954	5423	36	151
Lotus 21 F1	1961	949	37	26
Lotus 24 F1	1962	136	33	4
Stressed Skin and Monocoque				
Lotus 25 F1	1962	3254	32	103
McLaren F1	1966	1491	n/a	n/a
Lotus 79 F1	1979	4067	43	95
Lotus 79 F1	1979	6779	39	176
Lotus F1	1980	13558	34	399
Lola F1	1993	40675	36	1122
Backbone Type				
STP Indy Turbo car	1968	47454	62	765
Lotus Élan	1962	6101	34	180

**Appendix D. FEA CONTOUR PLOT OF CHASSIS WITH BATTERY
BOXES**



Please note: a scale factor applies to various member dimensions.